Deformation Optimization of Plate Heat Exchangers

Mattias Norén

DIVISION OF PRODUCT DEVELOPMENT | DEPARTMENT OF DESIGN SCIENCES
FACULTY OF ENGINEERING LTH | LUND UNIVERSITY
2016

MASTER THESIS

Deformation Optimization of Plate Heat Exchangers

How to Minimize Deformations in Gasket Plate Heat Exchangers

Mattias Norén

LUND
UNIVERSITY

Deformation Optimization of Plate Heat Exchangers

How to Minimize Deformations in Gasket Plate Heat Exchangers

Published by

Department of Design Sciences
Faculty of Engineering LTH, Lund University
P.O. Box 118, SE-221 00 Lund, Sweden

Subject: Machine Design for Engineers (MMK820)
Division: Product Development
Supervisor at the university: Per-Erik Andersson
Supervisor at Alfa Laval: Joakim Krantz
Examiner: Olaf Diegel

Abstract

The thesis was conducted in collaboration with Alfa Laval which is a global company operating in three key product areas: heat transfer, separation and fluid handling. One major product segment within the heat transfer area is the gasket mounted plate heat exchanger, which this thesis has focused on.

In a plate heat exchanger (PHE) the different mass flows are separated from each other with corrugated plates, made out of sheet metal. The key part of the plate is the heat transferring area which often consists of a wavelike pattern. When every other and other plate is rotated and mounted together contact points occur at the wave tops. When the equipment is pressurized deformations may occur in the contact points. The aim of the thesis was to understand how to optimize the wave pattern geometry to minimize the deformations.

The thesis was divided into three major parts: two parts with different simulation models and a third which consisted of laboratory experiments. The first simulation model was made with rough simplifications in order to obtain an automatized setup to scan a design space. The second simulation model was based on Alfa Laval's existing simulation procedure. It included more aspects to obtain realistic results, but was more time consuming since every simulation had to be prepared manually. This led to fewer simulated design points and each design point had to be chosen more carefully. The object of the experimental part was to validate the correctness of the simulation models.

The results showed that the geometry could be optimized in certain ways.

Keywords: Plate heat exchanger, optimization, finite element method, plate design, Alfa Laval.

Sammanfattning

Examensarbetet gjordes i sammarbete med Alfa Laval som är ett globalt företag verksamt inom tre huvudområden: Värmeöverföring, separering och flödeshantering. Ett av de största produktområdena inom värmeöverföring är packningsförsedda plattvärmeväxlare, vilket uppsatsen har fokuserat på.

I en plattvärmeväxlare hålls de olika massflödena separerade med hjälp av korrugerade plattor gjorda av plåt. Den viktigaste delen av plattan är den värmeöverförande ytan som består av ett vågfomat möster. När varannan platta vrids och plattorna monteras samman uppstår kontaktpunkter på vågtopparna mellan plattorna. När sedan utrustningen trycksätts kan det uppstå deformationer i kontaktpunkterna. Målet med uppsatsen var att förstå hur vågmönstret kan optimeras för att minimera dessa deformationer.

Uppsatsen delades upp i tre delar: Två olika simuleringsdelar och en tredje del som bestod av fysiska experiment. Den första simuleringsmodellen bestod av grova förenklingar för att kunna automatisera utforskningen av den uppställda konstruktionsrymden. Den andra simuleringsmodellen utgick från Alfa Lavals befintliga simuleringstillvägagångssätt. Den tar å ena sidan hänsyn till fler faktorer och uppnår på så sätt ett mer realistiskt resultat, men tar å andra sidan mer tid då alla förberedande steg måste göras manuellt. Detta resulterade i att färre utformningar kunde simuleras med denna metod och att valen av utformningspunkter blev allt viktigare. Den experimentella delen gjordes för att validera korrektheten av simuleringmodellerna mot verkligheten.

Resultaten visade att geometrin kan optimeras.

Nyckelord: Plattvärmeväxlare, optimering, finita elementmetoden, plattkonstruktion, Alfa Laval.

Preface

The Master Thesis has been conducted at the Department of Design Sciences, Faculty of Engineering LTH, Lund University as a collaboration with Alfa Laval.

I would like to thank my supervisor at Alfa Laval, Joakim Krantz, for his guidance during the work. I would also like to thank Håkan Larsson at the Mechanical Technology department at Alfa Laval for his advice.

At the university I would like to thank my supervisor, Lecturer Per-Erik Andersson for his support and cooperation throughout the thesis.

Lund, March 2016

Mattias Norén

Table of Contents

1 Introduction 15
1.1 The Company 15
1.2 Background 15
1.3 Ethics 17
1.4 Confidential Information 17
2 Aim 19
3 Method 21
3.1 Overview 21
3.1.1 Design Space Exploration 22
3.1.2 Forming and Pressure Simulations 22
3.1.3 Laboratory Experiments 22
3.2 Software 23
4 Limitations 25
5 Theory 27
5.1 Heat Exchangers 27
5.1.1 Function and Design of PHE 27
5.1.2 Manufacturing Process of Plates 29
5.1.3 Local and Global Deformation 29
5.2 Finite Element Method 30
5.2.1 Brief Explanation 30
5.2.2 Shell Elements and the Engineering Theory of Plates 31
5.2.3 Explicit and Implicit Solver 31
5.3 Anisotropic Material Model of Plasticity 32
6 Geometry 33
6.1 The Pressing Tool 33

6.2 Design Parameters 33
6.2.1 Constraints 34
6.2.2 Relations 35
6.3 Design Space 36
7 Design Space Exploration 37
7.1 Constraints 37
7.1.1 Geometry 37
7.1.2 Design Space 38
7.1.3 Model 40
7.2 Simulation Model Approach 41
7.2.1 Model 41
7.2.2 Material Model 42
7.2.3 Mesh 43
7.2.4 Boundary Conditions 45
7.2.5 Number of Contact Points 48
7.2.6 Friction 49
7.2.7 Other Adjustments 50
7.2.8 Zoomed in Study 50
7.2.9 Software interference 51
7.3 Post Process of Results 51
8 Forming and Pressure Simulations 53
8.1 Purpose 53
8.2 Constraints 53
8.2.1 Theoretical Plate Angle 53
8.2.2 Settings 54
8.2.3 Material Model 54
8.2.4 Global Deformation 54
8.2.5 Design Points 55
8.3 Simulation Model Approach 55
8.3.1 Model 55

8.3.2 Material Model 55
8.3.3 Boundary Conditions 56
8.3.4 Mesh 56
8.3.5 Forming Simulation 57
8.3.6 Pressure Simulation 57
8.4 Post Process of Results 59
8.4.1 Measurement 59
9 Laboratory Experiments 61
9.1 Constraints 61
9.2 Experimental Approach 61
9.2.1 Pressure Levels 61
9.2.2 Material 62
9.2.3 Measurement 63
9.2.4 Post Processing of Results 64
10 Results 67
10.1 Design Space Exploration 67
10.1.1 Initial Design Space Exploration 67
10.1.2 Zoomed in Study 69
10.2 Forming and Pressure Simulations 70
10.3 Comparison of Design Optimization Results 75
10.4 Laboratory Experiments 77
10.5 Verification of Simulation Models 78
11 Discussion 79
11.1 Design Exploration Simulations 79
11.2 Forming and Pressure Simulations 80
11.3 Laboratory Experiments 81
11.4 Comparison of Results 82
11.4.1 Verification of Simulation Models with Experiments 82
11.4.2 Design Optimization 82
11.5 General Improvements 83

11.6 Thoughts 83
11.7 Conclusions 87
11.8 Recommendations for Future Work 87
References 89
Appendix A Time Schedule
Appendix B Theoretical and True Plate Angle

1 Introduction

This chapter gives an introduction to the thesis. It includes a description of the company, the background of the project with a short brief of a plate heat exchanger and what problems that initiated the thesis.

1.1 The Company

Alfa Laval is a global company with three key product areas: heat transfer, separation and fluid handling. It all started in 1883 when Gustav de Laval and Oscar Lamm Jr founded the company Separator AB, which in 1963 became Alfa Laval. Today Alfa Laval holds more than 2000 patents, their products are sold in approximately 100 countries with 18,000 employees worldwide. In 2014 Alfa Laval had sales of 35.1 billion SEK. The head office is located in Lund, Sweden, which is also where the major part of the research and development of plate heat exchangers (PHE) is done [1].

1.2 Background

The key part of a plate heat exchanger (PHE) is the area where the major part of the heat transfer is supposed to take place, the heat transfer area. This part of the plate is often shaped in a wavelike arrow pattern, also called Chevron pattern, see Figure 1.1. Since every other plate is rotated the pattern creates contact points between the plates, see Figure 1.2. These contact points make sure the plates become a rigid structure when assembled.

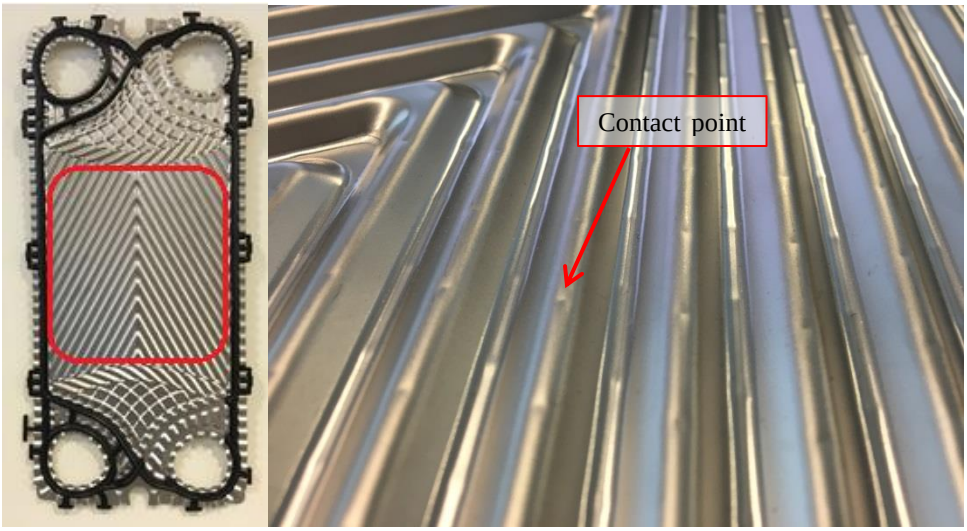

Figure 1.1. The heat transferring area marked and contact point deformations zoomed in

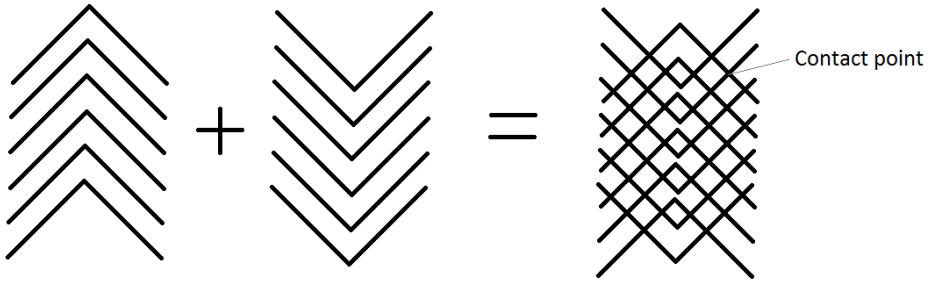

Figure 1.2. Schematic picture over contact points

Due to several design standards for pressure vessels such as ASME [2] and PED [3] the pressure vessel has to be tested and pressurized before it is taken into use. Alfa Laval pressurizes one of the two heat exchanger channels at a time after assembly. It is important to avoid deformations at this unsymmetrical load case since deformations can cause gaps between the plates which can lead to cracks and fatigue stresses when the equipment is operating. To increase the product performance large deformations needs to be avoided by an optimized design. A more detailed description of the function of a PHE can be found in chapter 5.

1.3 Ethics

There are no obvious ethical problems with heat exchangers compared with e.g. the weapon industry. In many applications heat exchangers are used to minimize the waste of energy in processes by preheating an incoming mass flow with an outgoing. Since energy production more or less always has a negative impact on the environment through emissions or exploitation of nature a minimization of the consumed energy for a certain process is positive. Since heat exchangers are general products with a broad spectrum of application areas it is up to the user to decide whether it is to be used for a good or bad cause. Despite this there are obvious situations where the reseller has a responsibility to make sure the equipment is not sold to e.g. terrorist organizations.

A heat exchanger can reduce the cost of a process, e.g. in the oil industry. In this sector the heat exchanger can be a contributing part in making it profitable to extract fossil oil which has a negative impact on the environment if it is combusted. However, a heat exchanger can contribute to making production of renewable energy more efficient and profitable which in the long term can reduce negative impact on the environment. In both cases the heat exchanger can reduce the waste of energy, which is positive. This argumentation strengthens that there are no ethical problems with working with development of heat exchangers.

1.4 Confidential Information

Some information regarding the Alfa Laval products such as material models, geometry and results were seen as confidential. This means that some parameter values could not be revealed and had to be presented in general terms. Some figures are not as detailed as they could have been and some scales have been removed or modified. In some places where it might look strange that no values are revealed there are footnotes marking the confidential information.

2 Aim

The general aim of the thesis is presented below.

The thesis was initiated to increase the knowledge of how different parameters affect the strength and deformation of the heat exchanger plates in contact points of the heat transfer area. The aim was to understand how to optimize the design to minimize the deformations. If no specific optimal design was obtained the objective was to find design guidelines on how to minimize the deformations.

It was of interest to investigate how different simulation models work and match the experimental results. The forming and pressure simulation routine was known to be functional but a more detailed verification against reality was of interest. The design space exploration simulations were known to be roughly simplified. It was still of interest to see how those kinds of simplifications would affect the results and if the method could be used in order to optimize the results by comparing them relatively to each other.

3 Method

This chapter describes the general and overall method of the thesis. More detailed simulation and experiment method descriptions are given in each subsection.

3.1 Overview

No conventional scientific overall method was used in the thesis. The method can rather be seen as a description of a product development procedure to obtain more information about the behavior of a product. Despite this, the well accepted Finite Element Method (FEM) was used as the main tool in solving the task. Other conventional engineering tools such as computational CAD-modulation and analytical mathematics were also used.

The thesis consists of three major parts. The two first parts handle different ways to model and simulate in a theoretical manner. The purpose of these simulations was to find an optimal design or at least a suitable design space. The third part was made to verify the theoretical models with laboratory experiments. A schematic picture of the thesis is seen in Figure 3.1.

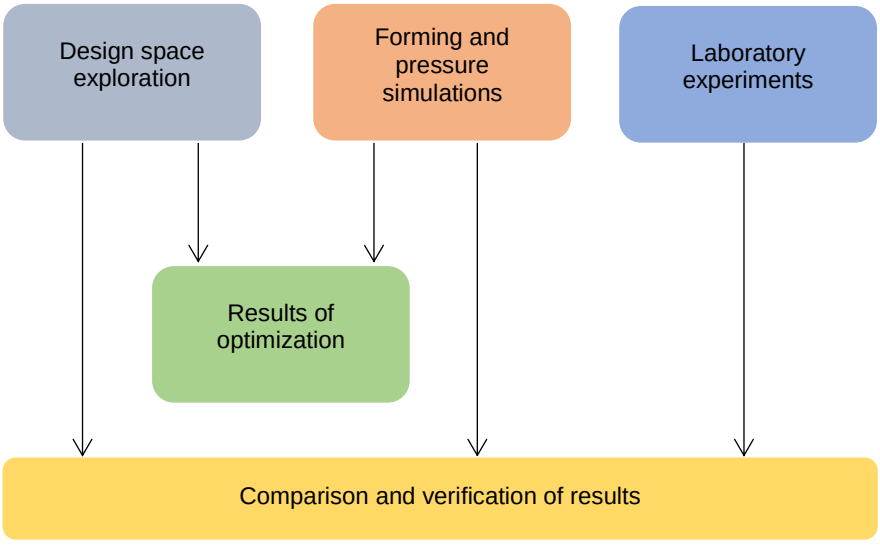

Figure 3.1. Schematic overview of the thesis

Each of the three major parts is described in more detail in separate chapters. Here follows a brief introduction to the three parts to make it possible to get an overview.

3.1.1 Design Space Exploration

This part of the thesis was made to explore the design space with a larger amount of design points than what was made in the forming and pressure simulation part. To be able to run all of the simulations within a reasonable time a lot of simplifications had to be made. The most important aspect was that the forming process was neglected and the geometry was controlled directly in the CAD software, Creo. A test matrix was set up and all the simulations could be run automatically from that. Ansys workbench was used to solve this FEM task. An existing Alfa Laval plate, further on denoted as "the reference plate", was simulated in two plate thicknesses to verify the model by laboratory experiments.

3.1.2 Forming and Pressure Simulations

With the results from the design space exploration some verifying simulations in the interesting design space area were performed. In this part, the forming process was included and also a more detailed material model was adopted. Each design point had to be manually prepared which made it more time consuming than the simulations in the design space exploration. The software used for this task was Creo and Dynaform for preparation of the model. Ls-dyna, which used an explicit solver instead of an implicit as Ansys did, was used to solve this FEM task. The difference between explicit and implicit solving method is described in the theory chapter. This simulation model was also used to simulate the reference plate in order to verify the model by laboratory experiments.

3.1.3 Laboratory Experiments

To verify the simulated results some experimental tests had to be done. Two different plate thicknesses of the reference plate were pressurized to four different pressure levels each, i.e. eight tests. The tests were made at Alfa Laval's laboratory in Lund. Afterwards, the results were compared to the simulations to see if the theoretical models were reliable.

3.2 Software

The software listed below was used in the thesis and all licenses were supplied by Alfa Laval.

- Creo 2.0
- Ansys workbench 16.0
- Dynaform 5.9.1
- LS-dyna
- Microsoft Word, Excel and Project 2010

4 Limitations

The limitations of the thesis are defined in this chapter.

Overall limitations for the thesis were made to achieve a well-defined project manageable within the time schedule. A Master Thesis time limit is one semester or approximately 20 weeks and as a consequence, the extent of the thesis must be restricted. The overall limitations are listed below:

- Only the mechanical aspects of the design were examined. This means no consideration of the heat transfer or flow aspects were evaluated even though they are affected by the design.
- Exclusively Chevron patterned heat transfer areas were investigated.
- Only contact points of the heat transferring area were investigated.
- The plate material was limited to stainless steel, Alloy 316.
- The interaction of two identical plates was investigated and accordingly plates with different Chevron angles were not mixed. However, the results may be applicable on a mixed setup.
- Shell elements were adopted in the simulation models.
- The geometry optimization simulations were performed with 0.5 mm in plate thickness.
- The verification of the simulation models made by laboratory experiments were implemented with both 0.5 mm and 0.4 mm plate thicknesses.
- The reference plate was used as a base in the modulation geometries.
- Only the reference plate's pressing depth, which is about 4 mm, was used.
- The reference plate was used to verify the theoretical model with reality through the laboratory experiments.

5 Theory

This chapter gives explanations of the mechanisms and theories which are fundamental to the thesis.

5.1 Heat Exchangers

There are several different types of heat exchangers such as tube or spiral heat exchangers but this thesis focus on plate heat exchangers (PHE). There are in general two types of PHEs, gasket mounted (GPHE) and brazed (BHE). In BHE all plates are brazed together and they cannot be disassembled to be cleaned or serviced. They are often used in smaller applications such as heat pumps or district heating systems in both private houses and apartment houses. GPHE are in general larger than BHE and are used when larger capacity is needed or possibilities of cleaning and servicing are important. Examples of applications for GPHE are: Chemical process industries, dairies, breweries, ships, greater buildings etc. This means that the media which is handled could be anything from corrosive acids, oil and seawater to milk and cream.

5.1.1 Function and Design of PHE

The purpose with a heat exchanger is to transfer heat energy from one media to another without mixing them together. PHE are made from corrugated plates which separate the flows from each other at the same time as they transfer the heat. The pattern of the corrugated plates are made to maximize the area, increase the flow turbulence, distribute the flows over the plates and separate the plates from each other to create flow channels. GPHE have gaskets as seal and the gaskets also make sure the flows are separated. The gaskets are most commonly attached at the edge of the plates but some gaskets need to be glued to stay attached when the equipment is assembled or opened. It is most common that the plates are in principal identical throughout the apparatus. Every other plate is rotated 180 degrees which makes half of the channels filled with warm and half with cold media, see Figure 5.1 and Figure 5.2. Outside of the heat transferring plates there are two thicker plates, frame and pressure plates, which hold the plate package together with bolts. Since the flows through the PHE are always more or

less pressurized (sometimes even vacuum occurs) the PHE must be considered as a pressure vessel. To avoid accidents there are standards which regulate and control how designing and testing is done. There are different standards around the world, e.g. ASME BPVC (American Society of Mechanical Engineers Boiler and Pressure Vessel Certification program) [2] is used in the US and the European Union has its own directive PED (Pressure Equipment Directive) [3].

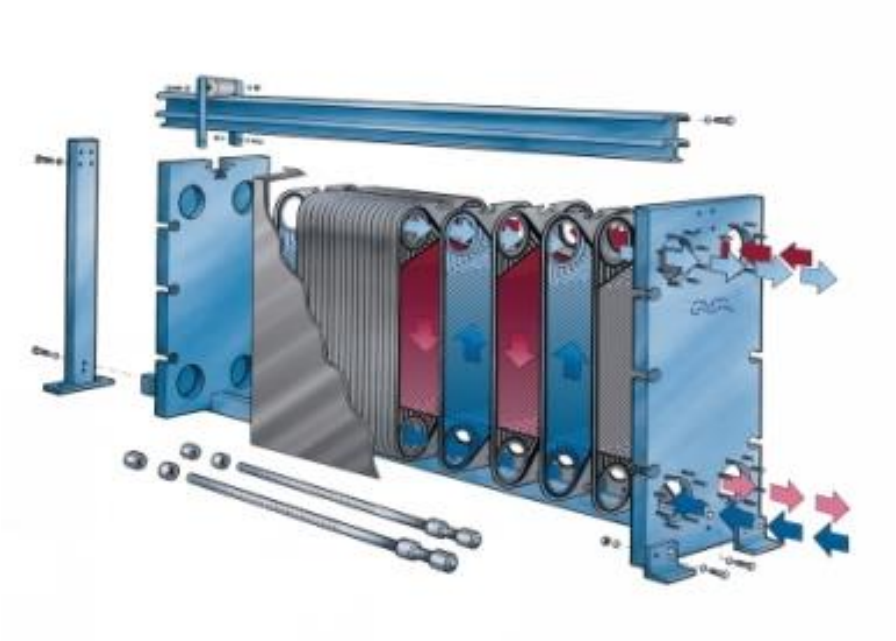

Figure 5.1. How a GPHE works [1]

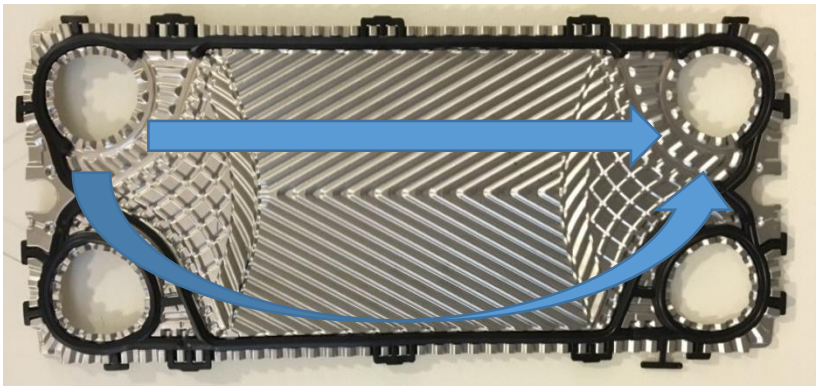

Figure 5.2. GPHE plate showing flow

The angle of the Chevron pattern, seen in Figure 5.3, is a parameter which affects both the flow and pressure drop through the PHE. It also has an impact on the mechanical properties since the angle affects the number of contact points. The angle is mainly between 30° and 60° and it is possible to mix plates with different angles.

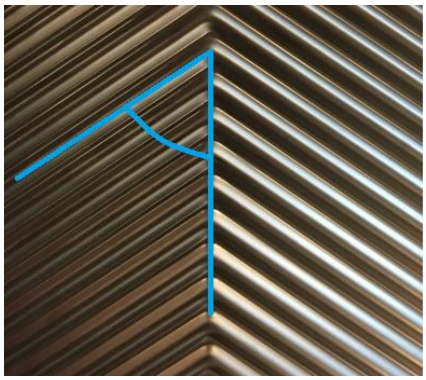

Figure 5.3. Angle of Chevron pattern

5.1.2 Manufacturing Process of Plates

A plate i.e. a plate for a specific product with a certain pressing depth is made from one pressing tool. The tool consists of two parts: a die and a stamp. The two tool parts are pressed together with sheet metal in between which is how the plates are formed. The same tool is used for different plate thicknesses and plate materials. This entails that compromises have to be made in the designing process to ensure the requirements can be achieved. The port holes can either be cut out before or after pressing. The forming method Deep Drawing, which means the plate is not locked at the edges, is used. The indentation becomes small in relation to the plate area, since the width and height dimensions are large in relation to the pressing depth.

5.1.3 Local and Global Deformation

Two different deformations of the heat transferring area could be evaluated. They were defined as the deformation difference between a contact point and a reference point, see Figure 7.22 and Figure 7.23. The local deformation considers the impact in the contact point. The global deformation considers both the impact in the contact point and the deformation impact of the whole plate. It was of interest to evaluate the difference between local and global deformation to see where the main deformation occured. Figure 5.4 shows a schematic picture of the measured values where all points are brought into the same plane. The

mathematical definitions of the global and local deformation are shown in Equation 1and Equation 2.

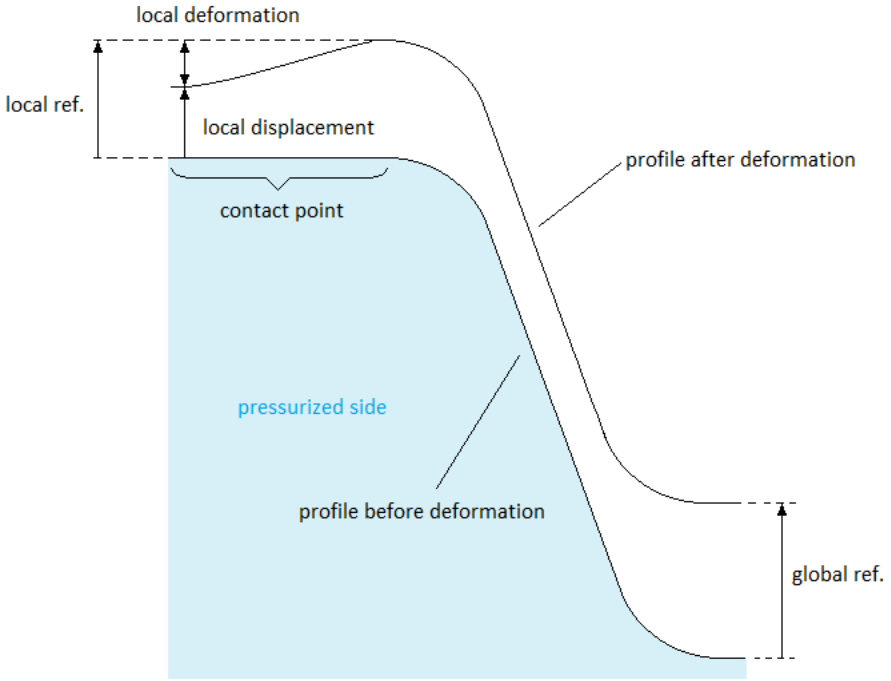

Figure 5.4 Explanation of measured values on plates

$$local\ def. = local\ ref - local\ disp. \tag{1}$$

$$global\ def. = (global\ ref. - local\ ref.) + local\ ref. - local\ disp.$$
$$\rightarrow global\ def. = global\ ref. - local\ disp. \tag{2}$$

5.2 Finite Element Method

5.2.1 Brief Explanation

Ottosen and Petersson write: "All the physical phenomena encountered in engineering mechanics are modelled by differential equations, and usually the problem addressed is too complicated to be solved by classical analytical methods. The *finite element method* is a numerical approach by which general differential equations can be solved in an *approximate* manner" [4]. The Finite Element

Method (FEM) is widely used for research and development applications. It is applicable in many fields and especially suitable to solve static and dynamic mechanical problems. To solve mechanical problems the geometry is needed. Most commonly the geometry is modulated with CAD software and imported to the numerical solving software. From the 3D model a mesh is generated to define the geometry in mathematical terms. A mesh is a grid system defined by elements and nodes. In mechanical applications one, two and three dimensional elements can be used. A material model can be needed to define the behavior of the elements if e.g. the deformation is of interest. Constraints which define the boundary conditions in some certain nodes are needed to obtain a solvable model.

5.2.2 Shell Elements and the Engineering Theory of Plates

For both of the simulation models used in the thesis shell elements were chosen instead of solid elements. Ottosen and Peterson write about shell elements in FEM: "…the theory of plates is an engineering approximation which reduces the original three-dimensional problem to a simpler two-dimensional problem. For many applications, however, this engineering theory provides realistic solutions, especially if the plate is thin." [4]. This means there will be no variation of the result over the thickness. They also write: "Generally speaking, a plate is a structure with a thickness *t* that is small compared with all other dimensions of the plate…" and "…a plate is loaded by forces normal to the plane of the plate." [4]. The ratio between plate thickness and other dimensions needed to assume The Theory of Plate is not specifically determined. The greater difference between thickness and other dimensions the better approximation will be obtained. Plates of PHE often have a thickness, *t*, smaller than a millimeter and the overall dimensions are in the scale of meters.

5.2.3 Explicit and Implicit Solver

Two different solving methods for the FEM differential equation were used for the simulation models, explicit and implicit method. The design space exploration simulation model which was solved with Ansys used the implicit method. The more complex model, which included the plate forming, used the explicit method by the software of Ls-dyna. Some practical information about the differences between explicit and implicit solver were found on the Ls-dyna support webpages:

"In nonlinear implicit analysis, solution of each step requires a series of trial solutions (iterations) to establish equilibrium within a certain tolerance. In explicit analysis, no iteration is required as the nodal accelerations are solved directly." [5].

"The time step in explicit analysis must be less than the Courrant time step (time it takes a sound wave to travel across an element). Implicit transient analysis has no inherent limit on the size of the time step. As such, implicit time steps are generally several orders of magnitude larger than explicit time steps." [5].

"Explicit analysis handles nonlinearities with relative ease as compared to implicit analysis. This would include treatment of contact and material nonlinearities." [5].

"Implicit analysis requires a numerical solver to invert the stiffness matrix once or even several times over the course of a load/time step. This matrix inversion is an expensive operation, especially for large models. Explicit doesn't require this step." [5].

5.3 Anisotropic Material Model of Plasticity

The sheet metal gets anisotropic material properties caused by the forming process. Therefore an anisotropic material model was adopted in the forming and pressure simulations. The model was based on a planar-stress yield criterion for orthotropic anisotropy which Barlat and Lian presented in 1989, shown by Equation 3, 4 and 5. [6].

$$f = a|K_1 + K_2|^M + a|K_1 - K_2|^M + c|2K_2|^M = 2\bar{\sigma}^M \tag{3}$$

Where:

$$K_1 = \frac{\sigma_{xx} + h\sigma_{yy}}{2} \tag{4}$$

$$K_2 = \sqrt{\left(\frac{\sigma_{xx} - h\sigma_{yy}}{2}\right)^2 + p^2\sigma_{xy}^2} \tag{5}$$

$\bar{\sigma}$ is the uniaxial yield stress in the rolling direction

M is a material coefficient e.g.:

$M = 6$ for a BCC material (Body Center Cubic structure)

$M = 8$ for a FCC material (Face Center Cubic structure).

a, c, p and h are material constants which can be calculated from R values obtained from uniaxial tension tests in three directions, for instance R_0, R_{45} and R_{90}. The R values are ratios between strains in two directions. For more details see the article by Barlat F. and Lian J. [6]

6 Geometry

This section examines the geometry and conditions that have to be taken into account when modulating and simulating. All equations are derived from the geometry.

6.1 The Pressing Tool

It is important to remember that the plates are manufactured by a pressing procedure. This means that the design engineers control the plate design through the pressing tool. In Figure 6.1 the pressing tool is displayed with a plate in between the two tool parts.

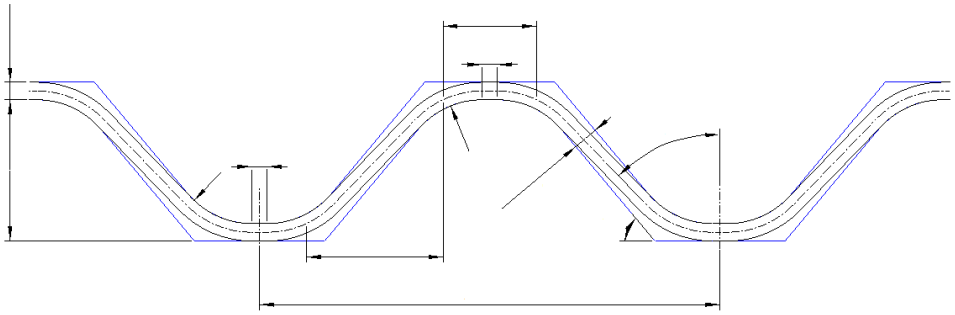

Figure 6.1 Pressing tool and plate

6.2 Design Parameters

The cross section of the heat transfer area is set up by several parameters. The geometry together with the constraints gives a system of two degrees of freedom and which parameters to become the design parameters can be chosen. The geometry in Figure 6.1 is symmetric in the vertical direction and periodic in the horizontal direction. In Figure 6.2 the parameters are denotation described.

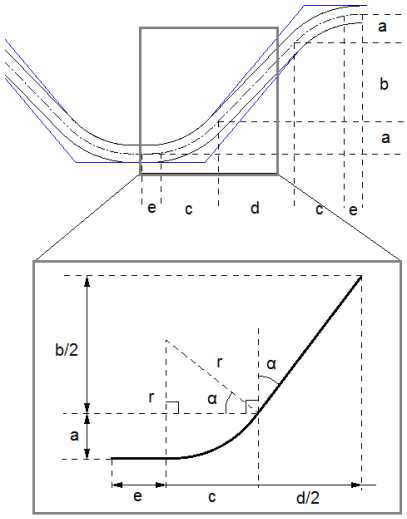

Figure 6.2. Denotation of geometry. The zoomed in area shows the center line of the plate.

There are seven parameters:

- r – radius
- α – angle
- a – distance
- b – distance
- c – distance
- d – distance
- e – distance

Note that the parameters refer to the centerline of the plate. There are two constants to be decided:

- h – height or depth of tool
- ξ – line elongation

6.2.1 Constraints

The constraints are defined from the two constant parameters above. First consider the plate depth which is assumed to be equal to de tool depth (h) and the definition is given by Equation 6.

$$h = 2a + b \tag{6}$$

Secondarily the line elongation (ξ), i.e. how much larger the plate surface is after deformation compared to before deformation, is given by Equation 7.

$$\xi = \frac{e + r\pi\frac{90-\alpha}{180} + \frac{b}{2\cos\alpha}}{e + c + \frac{d}{2}} \tag{7}$$

6.2.2 Relations

From Figure 6.2 Equations 8 and 9 can be derived.

$$a = r(1 - \sin\alpha) \tag{8}$$

$$c = r\cos\alpha \tag{9}$$

Equations 6 and 8 combined gives Equation 10.

$$b = h - 2a = h - 2r(1 - \sin\alpha) \tag{10}$$

The geometry in Figure 6.2 also gives Equation 11.

$$d = b\tan\alpha = \big(h - 2r(1 - \sin\alpha)\big)\tan\alpha \tag{11}$$

Equation 7 with inserted expressions from Equations 9, 10 and 11 gives Equation 12.

$$\xi = \frac{e + r\pi\frac{90-\alpha}{180} + \frac{b}{2\cos\alpha}}{e + c + \frac{d}{2}} = \frac{e + r\pi\frac{90-\alpha}{180} + \frac{\frac{h}{2} - r(1-\sin\alpha)}{\cos\alpha}}{e + r\cos\alpha + \left(\frac{h}{2} - r(1-\sin\alpha)\right)\tan\alpha} \tag{12}$$

Equation 12 can be described either as a function $r(e, \alpha)$ (Equation 13) or as a function $e(r, \alpha)$ (Equation 14).

$$r = \frac{\frac{\frac{h}{2}}{\cos\alpha} - (\xi - 1)e - \xi\frac{h}{2}\tan\alpha}{\xi(\cos\alpha - (1-\sin\alpha)\tan\alpha) - \pi\frac{90-\alpha}{180} + \frac{1-\sin\alpha}{\cos\alpha}} \tag{13}$$

$$e = \frac{r\pi\frac{90-\alpha}{180} + \frac{\frac{h}{2} - r(1-\sin\alpha)}{\cos\alpha} - \xi\left(r\cos\alpha + \left(\frac{h}{2} - r(1-\sin\alpha)\right)\tan\alpha\right)}{(\xi - 1)} \tag{14}$$

Now an equation system with two degrees of freedom is obtained from the seven parameters and the five equations, 8 to 12. When choosing which parameters to be free, i.e. the design parameters, there are some alternatives. The flat surface e, the radius r, and the angle α are all possible, but only two can be chosen. It was seen that it was easiest to graphically interpret the design space as a function of radius and angle and therefore they were chosen as design parameters.

All equations were verified by CAD-models and drawings, i.e. known design parameters from an existing plate where the input and the output were compared to the existing plate.

6.3 Design Space

It is the variation of the design parameters that sets the border of the design space. Since there are two degrees of freedom a design space of two dimensions follows. When displaying the design space it is easy to see it as a result of a varying radius and angle, see Figure 6.3. It is limited to positive distances, radius and angle leading the design space to be constrained between the two curves and the positive axes. Within the design space, parameter e and b are varying as follows:

$0 \leq e \leq e_{max}$ mm*

$0 \leq b \leq b_{max}$ mm*

The whole theoretical design space is displayed in Figure 6.3 constrained by Equation 10 and Equation 13.

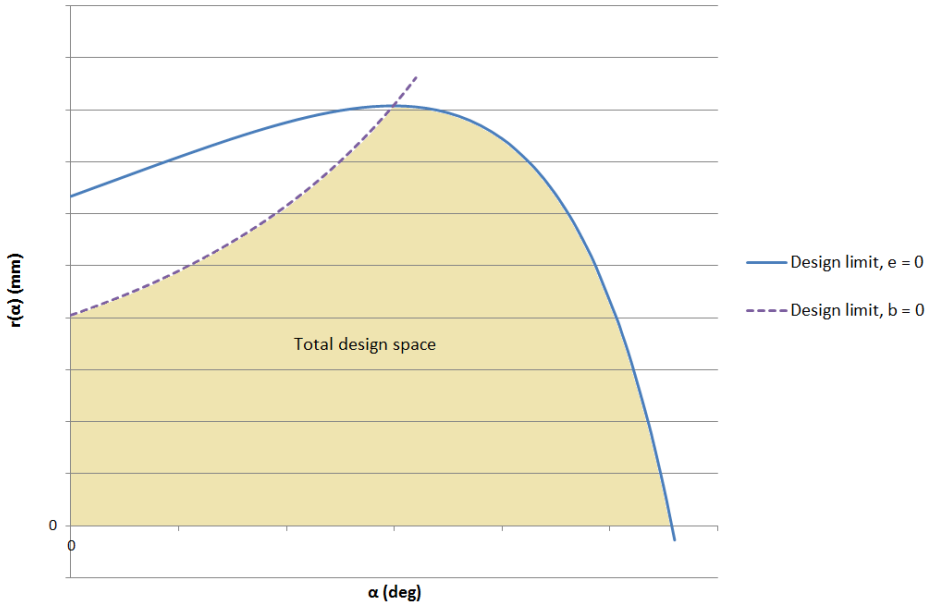

Figure 6.3. Total design space

* Confidential Alfa Laval information

7 Design Space Exploration

The design space exploration part of the thesis aimed to get a brief picture of the deformation behavior over the interesting part of the design space. The interesting part of the design space refers to the part which is reasonable to manufacture and design. The aim was to get results for several design points to be able to plot the results over the design space. This would make it possible to see which area could be interesting for further investigations. It also aimed verify the simulation model with the laboratory experiments

7.1 Constraints

7.1.1 Geometry

The plate depth that was chosen to use was equal to the reference plate depth[*]. Inserted in Equation 6 it gave Equation 15.

$$2a + b = h_{ref.} \text{ mm} \tag{15}$$

The line elongation was set to a value which was common for Alfa Laval's plates, $\xi_{com.}$[*]. Inserted in Equation 7 it gave Equation 16.

$$\frac{e + r\pi\frac{90 - \alpha}{180} + \frac{b}{2\cos\alpha}}{e + c + \frac{d}{2}} = \xi_{com.} \tag{16}$$

The line elongation value was selected before the reference plate line elongation value was known. Therefore, the verifying simulations were run with a different line elongation than and the design space exploration and forming and pressure simulations. The values differed one percent unit and did not affect the results since no comparison were made between them.

[*] Confidential Alfa Laval information

The Chevron angle was set to 60° which meant that the model both represented an angle of 60° and 30° at the same time, since $90° - 60° = 30°$.

7.1.2 Design Space

In discussion with design engineers at Alfa Laval the design space parameters α and r were preliminary limited as:

$\alpha \geq \alpha_1{}^\circ$

$r \geq r_1\, mm$

These boundaries took into account a reasonable design in manufacturing and mechanical aspects. It also gave extra design space which could make it possible to discover what happens outside the existing guidelines and recommendations. Initially eight design points were chosen to cover the selected design space. They were placed to give as much information as possible about the different parameters, see Figure 7.1.

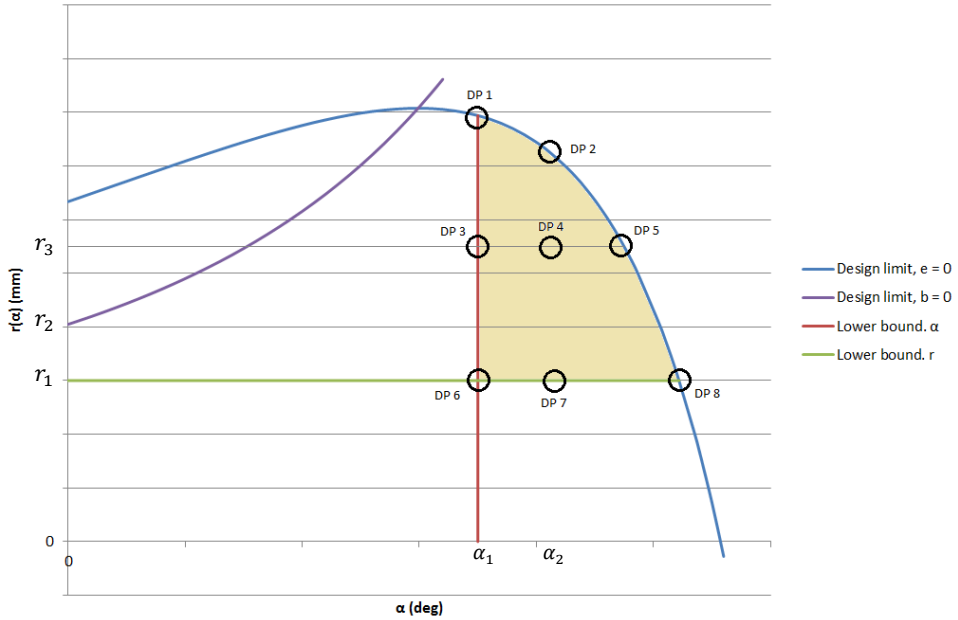

Figure 7.1. Selected design space

The design points were selected with the full factorial Central Composite Design (CCD) in mind, but had to be adapted to this specific case. Some of the design points were slightly moved from the boundaries to make sure they were solvable. Some of the design points on the boundaries of the design space can be seen in Figure 7.2 to Figure 7.6.

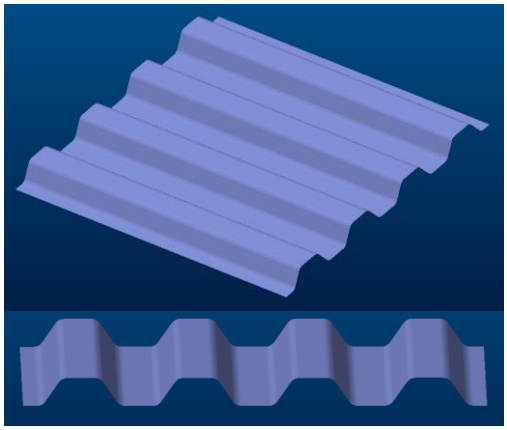

Figure 7.2. Design point 6

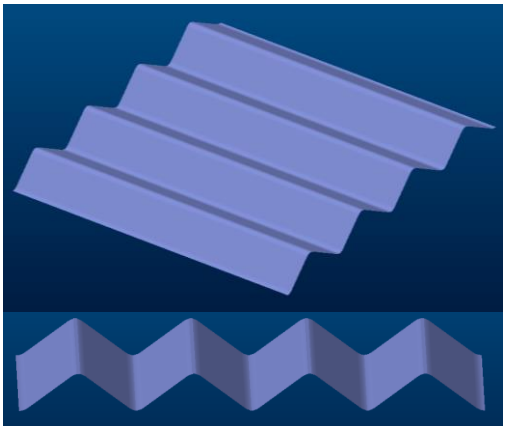

Figure 7.3. Design point 8

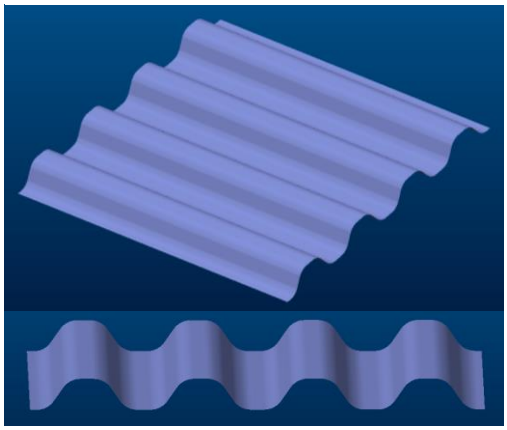

Figure 7.4. Design point 3

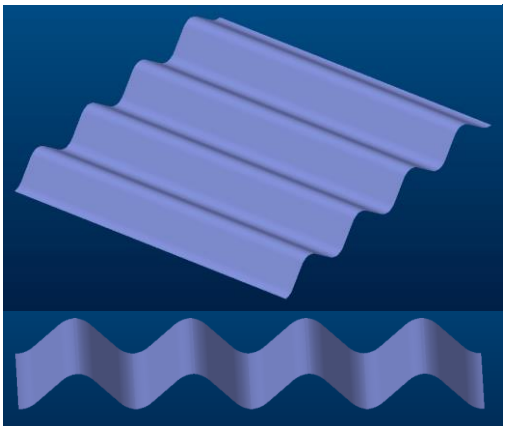

Figure 7.5. Design point 5

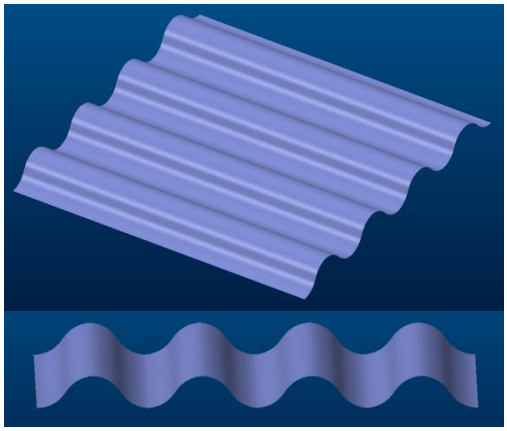

Figure 7.6. Design point 1

After the results of the first design exploration were obtained further studies were made. To see where a possible optimum could be the design points for the zoomed-in study were selected more arbitrarily step by step as the results were obtained. This is why the design points were not evenly distributed.

7.1.3 Model

The hydrostatic pressure difference between the upper and lower part of the channels caused by the gravitation was neglected i.e. a homogeneous pressure was applied.

Effects from the forming process were neglected since the model was modulated directly in CAD. This means that there were no internal stresses or local thinning of the plate caused by the forming process, which probably has a significant impact on the results. This simplification is further discussed in chapter 11.

The plates in a GPHE are pressed together by a frame with bolts. When mounted together an initial pressure on the plates and gaskets is created. After a while the pressure decreases due to relaxation of the gaskets but there will always be a remaining built in pressure. This pressure was neglected in these simulations.

7.2 Simulation Model Approach

Due to the fact that the study is a design space exploration a large amount of simulations were planned. To do this within an acceptable calculation time with the available computer capacity some simplifications had to be made. To decide how the model could be set up, several investigations and test simulations had to be made; thus a way of how evaluating the results also had to be defined.

7.2.1 Model

A cut out of two plates on top of each other was made as seen in Figure 7.7. This means one plate had the wave pattern along the sides and one had it rotated relative to the sides, also seen in Figure 7.7.

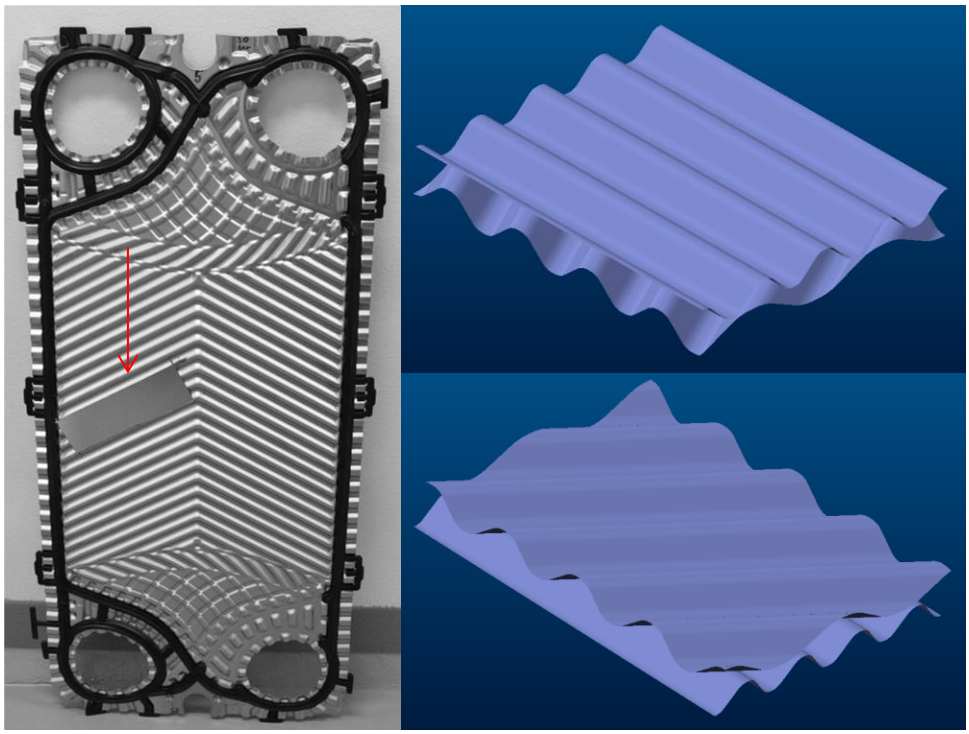

Figure 7.7. Cut out section which was measured and the model in CAD in two different views

The plates were modulated directly in Creo parametric 2.0 CAD system. The model consisted of two shells which were placed on top of each other with a distance of a calculated plate thickness from each other. The plate thickness was modified with the line elongation factor. The plate thickness in the CAD was calculated according to Equation 17.

$$\textbf{plate thickness} = \frac{\textbf{0.5 mm}}{\xi_{com.}} \tag{17}$$

The thickness for the verifying simulations was calculated in the same way.

As already mentioned, it was decided that the model would consist of shell elements instead of solid element since the thickness was considered negligible in relation to the area of the plate. With shell elements there is no variation of the results in the thickness direction and this was considered to be an acceptable simplification.

7.2.2 Material Model

The simulated material was stainless steel alloy 316 with data from Alfa Laval, see Table 1 and Figure 7.8. It was modulated with isotropic material behavior assumed.

Table 1. Material properties used in Ansys

Material properties	
Young's modulus, E	200 GPa
Poisson's Ratio, *v*	0.3

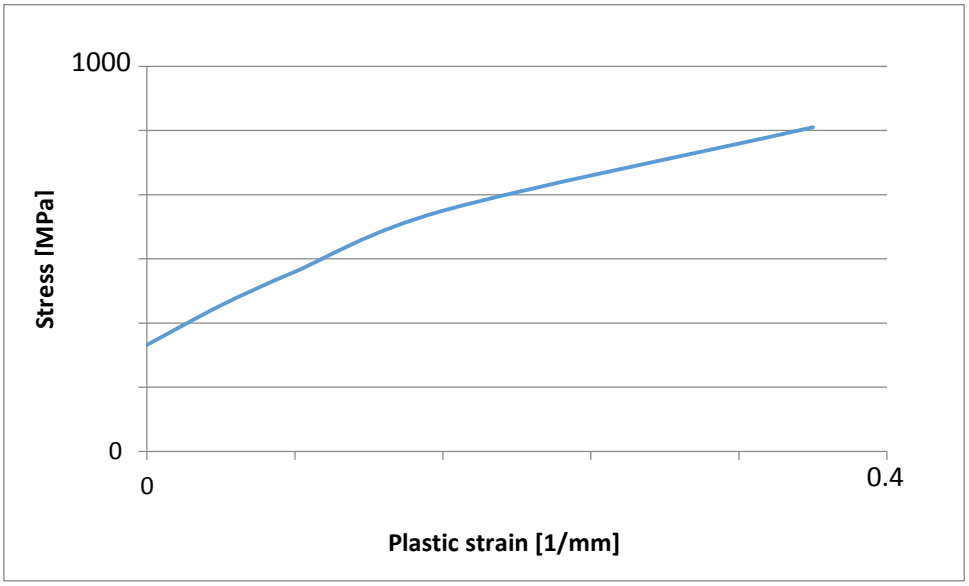

Figure 7.8. Plastic strain/Stress plot used in Ansys

7.2.3 Mesh

To determine which mesh size to use different sizes were tested and the results were evaluated. To minimize the solving time, it was decided that a finer mesh would be adopted in the contact areas between the two plates than in the rest of the model. For this purpose the contact sizing tool in Ansys Mechanical was used applied at the contact surfaces as seen in Figure 7.10. The settings in Figure 7.9 were used for the overall mesh at all time.

Details of "Mesh"

Display	
Display Style	Body Color
Defaults	
Physics Preference	Mechanical
Relevance	0
Sizing	
Use Advanced Size Function	On: Curvature
Relevance Center	Medium
Initial Size Seed	Active Assembly
Smoothing	Medium
Span Angle Center	Medium
Curvature Normal Angle	Default (30.0 °)
Min Size	1.e-004 m
Max Face Size	5.e-003 m
Growth Rate	Default
Minimum Edge Length	8.9068e-004 m

Figure 7.9. Over all mesh settings

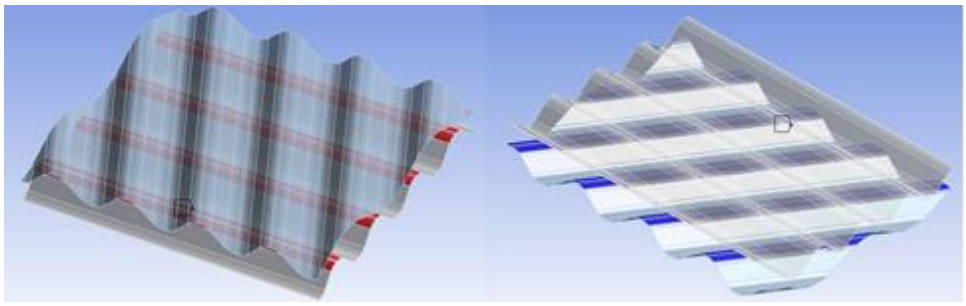

Figure 7.10. Contact surfaces

Figure 7.11 and Figure 7.12 shows different contact mesh sizes.

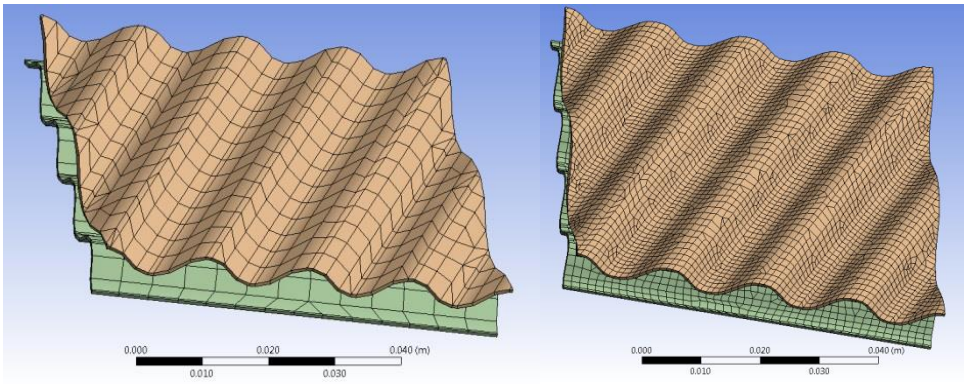

Figure 7.11. Contact mesh size 5 mm and 1 mm

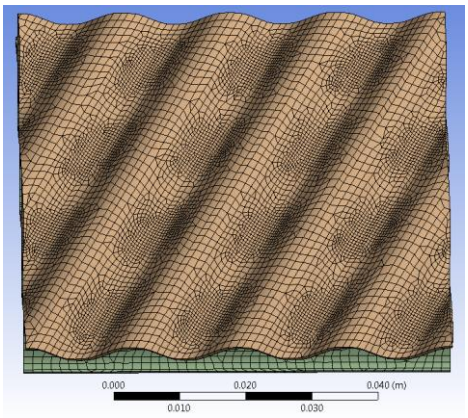

Figure 7.12. Contact mesh size 0.5 mm

.
Figure 7.13 shows the different contact mesh sizes that were tested and which results were achieved.

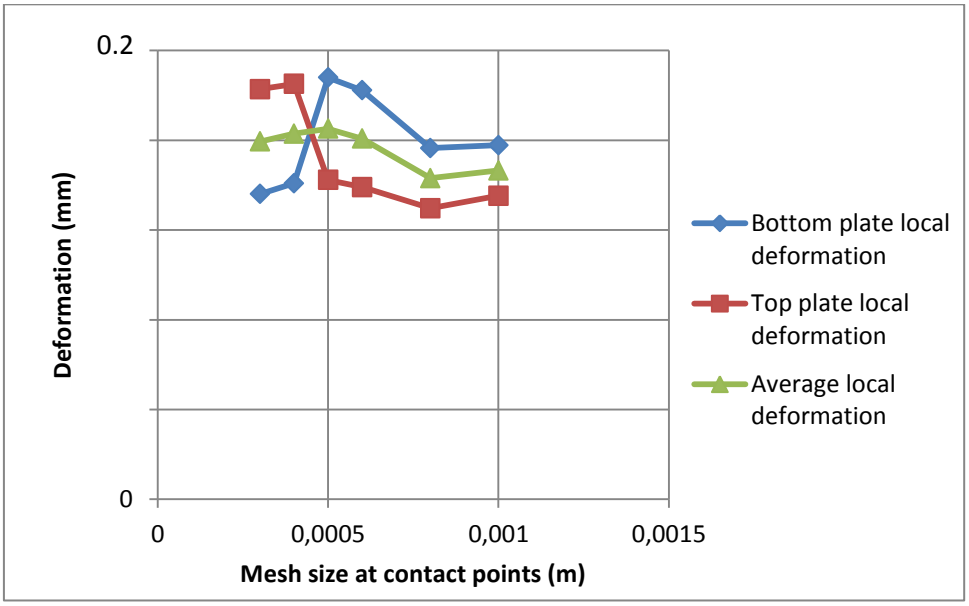

Figure 7.13. Results different mesh sizes

It could be seen that something happened at 0.5 mm's mesh size. It seemed like the results of the two plates had switched places which can be a result of instabilities in the numerical model. It was decided that 0.5 mm would be a good mesh size to begin with since it seems like the sum of the deformation of the two plates stabilizes beyond this point. With a smaller mesh size the calculation time increases rapidly and 0.5 mm was considered to be a good compromise.

7.2.4 Boundary Conditions

The simulated sample was not located near the plate edges, which entails that the surrounding geometry constrains the sample edges from moving. Therefore, it was assumed that the sample edges could be constrained as locked.

When deciding the boundary conditions it was important to keep in mind that the heat transferring area contains a great number of contact points. Therefore the analysis would consider a cutout of points that were located far from the edges of the real plate. To make sure the boundary conditions did not affected the simulated results more than necessarily there had to be at least one layer of contact points between the measured ones and the boundaries e.g. as in Figure 7.14.

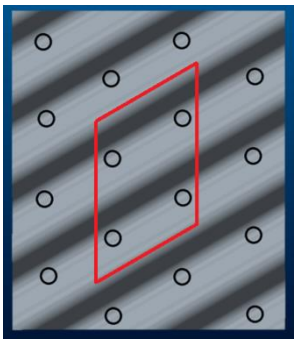

Figure 7.14. 16 contact points. The marked ones were used for measuring results

Figure 7.15 shows the boundary condition model tree.

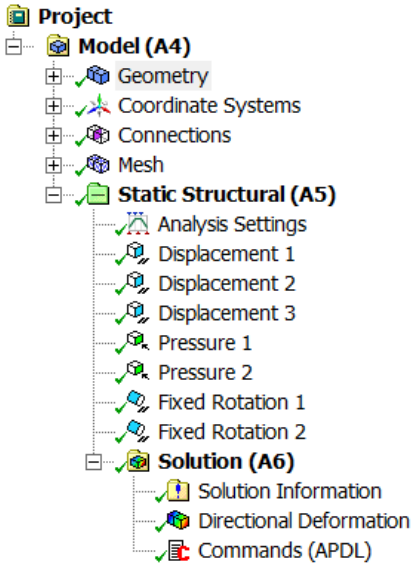

Figure 7.15. Boundary conditions and outer loads

The sides of the plates, as seen in Figure 7.16, were constrained not being able to move in the normal direction to each side. For each side the rotation around the axis along the side was also fixed.

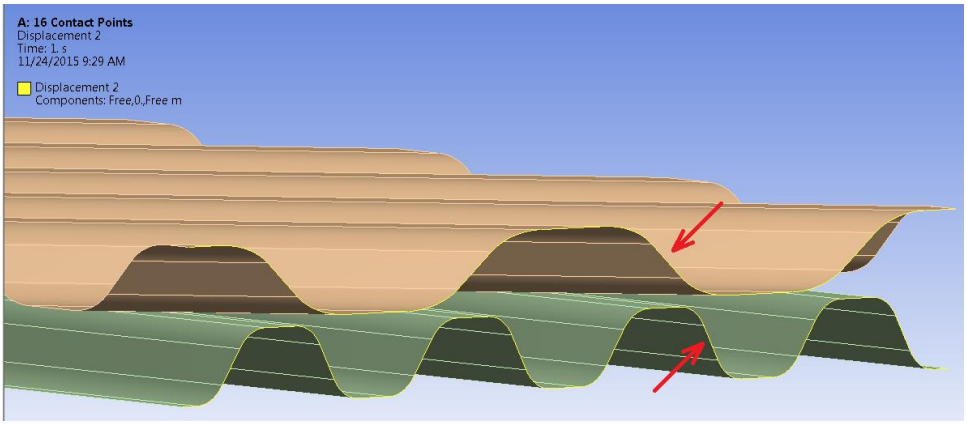

Figure 7.16. Sides marked with arrows

The top plate was fixed in z-direction in each corner, see Figure 7.17.

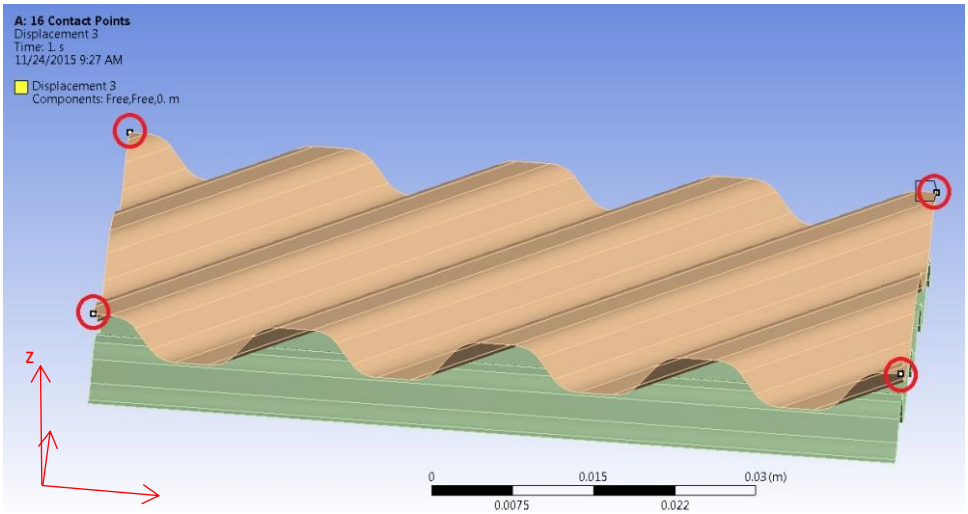

Figure 7.17. Corner deformation fixed in z-direction

The pressure was ramped up from zero in the first load step and ramped down again in the second and last load step. This was done simultaneously at both plates in opposite direction. The pressures were applied normal to plate curvature as seen in Figure 7.18.

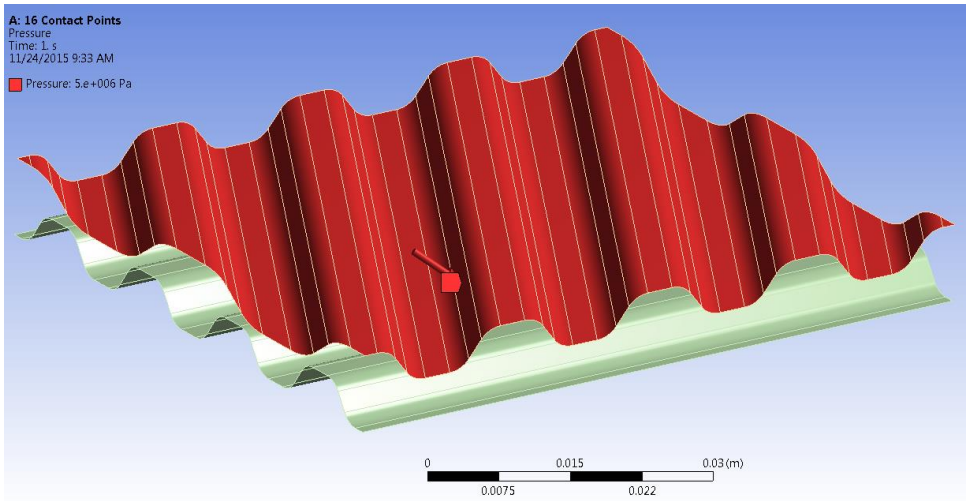

Figure 7.18. Pressure on top plate

7.2.5 Number of Contact Points

How many contact points the model should consist of had to be decided. It was of interest to simulate as few contact points as possible to achieve more efficient calculations, but enough to gain a realistic result. Different numbers of contact points were tested to get a clue to how it would affect the results, see Table 2.

Table 2. Different numbers of contact points that were tested

Total number of contact points	Number of contact points for evaluation of the average results
9	1
16	4
25	9
36	4

The choice of 50 barg as pressure was arbitrarily made after having a brief look at test pressures for different apparatus. The test pressures for the design exploration simulations were more carefully chosen.

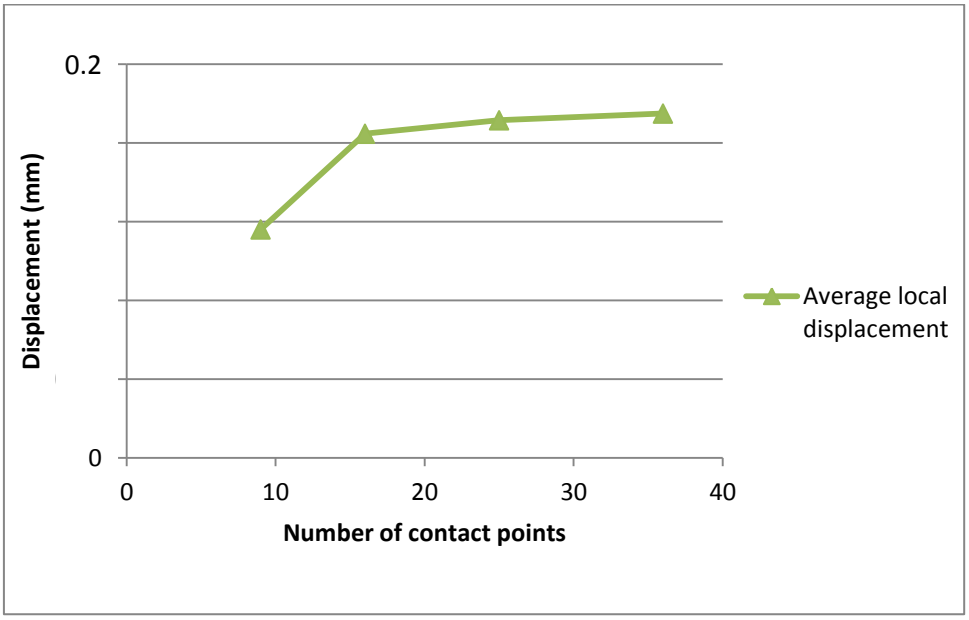

Figure 7.19. Test of different numbers of contact points at 50 barg

The result was used since it seemed to converge over approximately 16 contact points.

7.2.6 Friction

Since the outer forces (the pressures) were only applied normal to the plates, the internal friction forces were assumed to be close to zero. However, friction forces may have appeared due to shearing caused by the local deformation. Different friction coefficient values were tested but the actual value could be larger than the tested ones. In the manufacturing process the plates are lubricated before pressing and washed before being assembled. Due to Figure 7.20 it seemed as though the friction coefficients did not have any major impact on the results, therefore they were neglected.

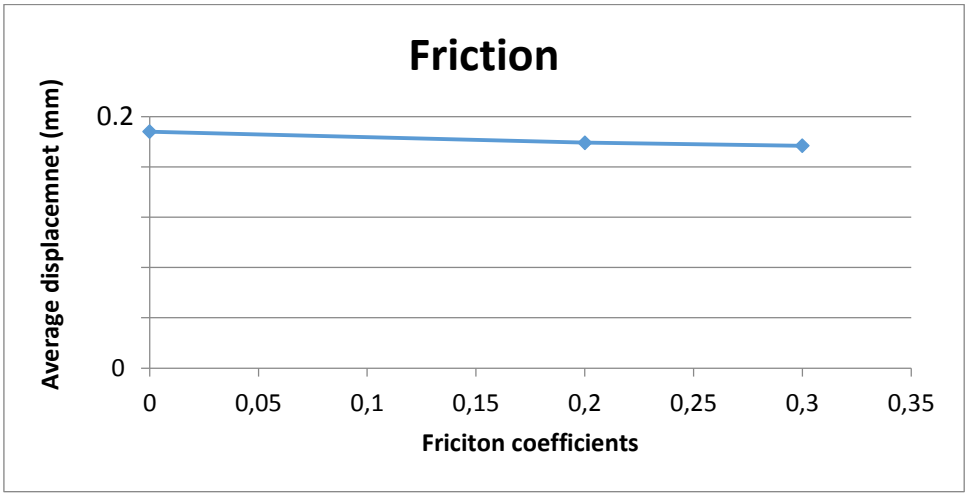

Figure 7.20. Friction coefficients at 50 barg

7.2.7 Other Adjustments

The mesh adjustment "midside nodes" allows quadratic elements instead of linear. This may increase the accuracy of the simulation but it also increases the solving time. Some simulations where run to evaluate the differences and influence of this adjustment but the result did not significantly differ.

To make the simulation converge more easily the time steps were set manually to be allowed to vary between 20 and 300 sub-steps with an initial value of 20 sub-steps.

7.2.8 Zoomed in Study

When the first design space exploration was made the interesting areas were selected for further investigation. These areas or lines were the radiuses r_1, r_2, r_3 in the design space chart, see Figure 7.1. The existing design points were also reused here. Since the line r_2 was in the middle of the interesting area in between the initial design points it was investigated in the most detail i.e. with most design points. Firstly a number of equally distributed design points were evaluated over the line, secondly design points where chosen more arbitrarily where there seemed to be a minimum or maximum.

7.2.9 Software interference

The geometry in Creo was made to be controlled by relations based on the previously described geometry equations. This means that the geometry could be controlled completely by the two parameters radius and plate angle. In Ansys workbench a test matrix was made with different parameter values. The two different types of software were connected and the geometry could be modified for each simulation from the test matrix in Ansys. No manual interference was needed.

7.3 Post Process of Results

When post processing results it is preferable to make the different simulations easy to compare and ideally find one comparable value for each test. It was possible to measure the deformation over one single contact point, but due to local variations the result may differ slightly over the contact points. To make the results more reliable four contact points were measured and an average value was calculated.

To get the wanted data a script, "command script", for Ansys was programmed. The script was inserted in the model tree as seen in Figure 7.21. The script found the center of the contact and reference points and extracted the deformations in the z-direction (normal to the undeformed plate). The four contact points and local and global reference points can be seen in Figure 7.22 and Figure 7.23.

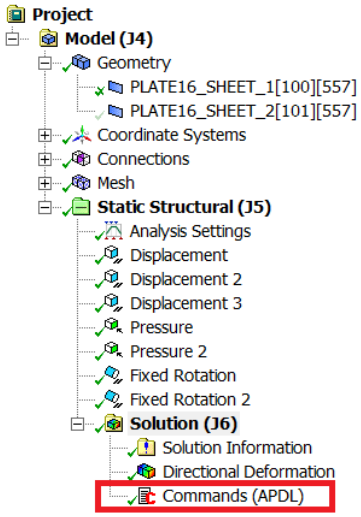

Figure 7.21. Command script in the model tree

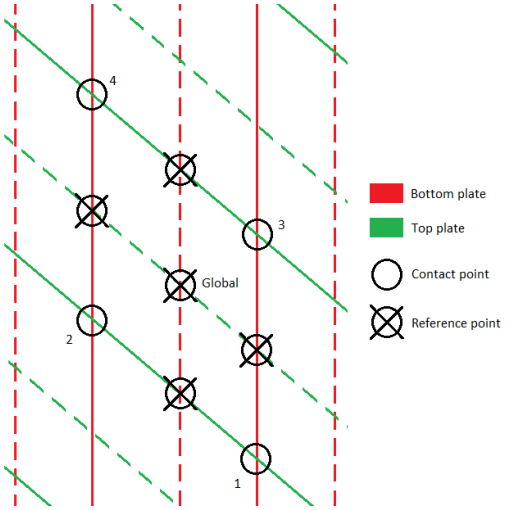

Figure 7.22. Points for measurement of results

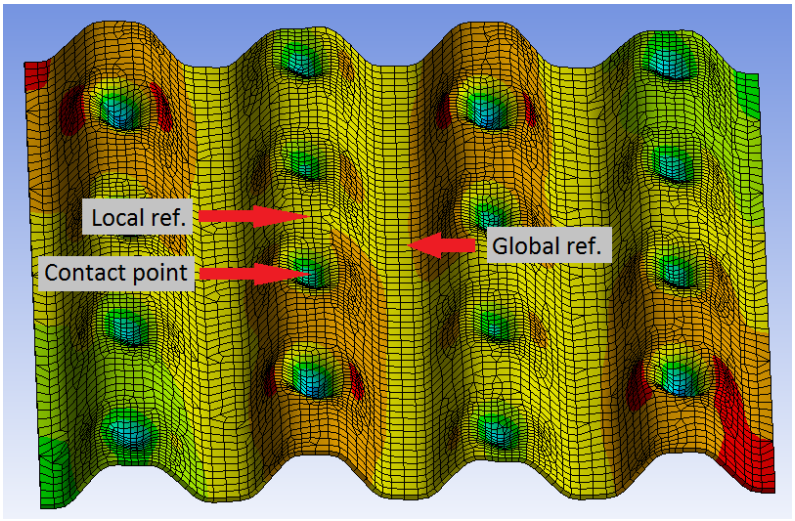

Figure 7.23. 3D view of points of interest on the bottom plate with exaggerated deformations

When a simulation was made the script was run and the results were exported to a text file. The text file was manually exported to a preprogrammed Excel file which calculated the post processing calculations. For both bottom and top plate a local deformation value and a global deformation value were calculated for each contact point. Average values were calculated over the contact points to get one value for each plate and type of deformation and a total average value was also calculated for the two plates. All results are displayed in chapter 10.

8 Forming and Pressure Simulations

The Forming and Pressure Simulations were based on a simulation routine that Alfa Laval uses to evaluate new plate tools and plates. This simulation routine uses the LS-Dyna FEM solver which in this case uses an explicit solver, unlike the implicit solver which Ansys ordinarily uses.

8.1 Purpose

The aim with these simulations was to verify or dismiss the findings from the design space exploration simulations. This simulation method includes the plate forming process; hence, it is more realistic. The method was not used for the design space exploration simulations because it is much more time consuming since each simulation has to be manually prepared for all steps from CAD to forming and pressure simulation. Since this simulation routine is used by Alfa Laval in development of plates it was of interest to see how the results would differ from the other simulation model and also from reality in terms of the laboratory experiments.

8.2 Constraints

8.2.1 Theoretical Plate Angle

In the design exploration simulations the plate was directly modulated and therefore all parameters could be controlled precisely. When the tool was modulated instead of the plate the aim was to obtain the theoretical plate parameters. The real values, e.g. plate angle would differ a bit since the theoretical value assumes a homogenous, undeformed plate thickness. In reality the thickness decreases as a consequence of the forming and this will cause a different plate angle. The tool angle and plate angle also differs, since the tool is made to press multiple plate thicknesses. The difference between plate angle and tool angle can be seen in Figure 8.1.

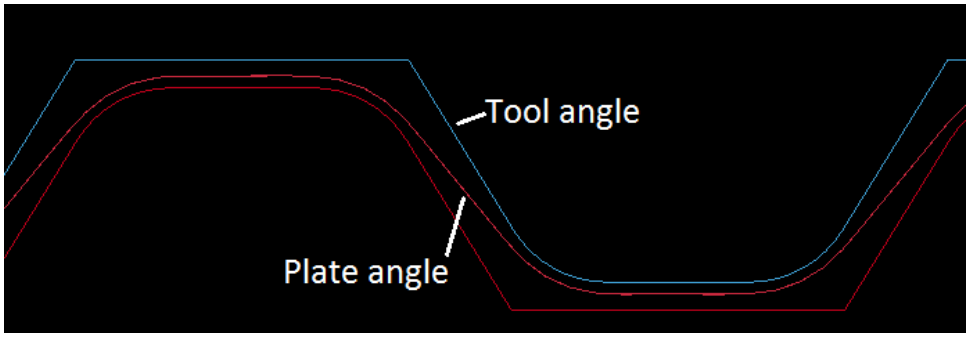

Figure 8.1. Theoretical plate angle shown by the plate middle line

8.2.2 Settings

Since the thesis was limited in time different settings such as mesh size etc. were not evaluated and tested. Instead the setting was made with Alfa Laval's existing guidelines. This means that Alfa Lava's guidelines also could be evaluated.

8.2.3 Material Model

The material model that Alfa Laval uses for forming and pressure simulations includes anisotropy caused by the rolling process of the sheet metal. This is particularly important when titanium is simulated since it is more anisotropic than stainless steel. This was neglected since it was not obvious how to place the tools in correct positions relative to the directions of the material combined with the minor impact of the anisotropy of stainless steel. Therefore, the direction of the material was only oriented by the global coordinate system of the model and not rotated to fit the tool more realistic.

8.2.4 Global Deformation

The design exploration simulations showed that the global deformation was almost the same as the local deformation. This means that the total deformation of the plate is mainly caused by the local deformation. The simulations also showed that it was difficult to measure the global deformation after the pressure simulations with a satisfying accuracy; hence, it was decided that the global deformation would not be included in the further analysis.

8.2.5 Design Points

It was of interest to investigate the radius which was examined in most detail in the design exploration study, i.e. r_2 in Figure 7.1. The radius r_3 was also of interest to investigate since it was quite close to the radius used in the reference plate.

8.3 Simulation Model Approach

The method which was used is the same as Alfa Laval uses when developing plates and it consists of two major steps. Firstly the plate forming simulations were made, in this case one for each plate. Secondarily the formed plate with all internal stresses and other information was assembled in a pressure simulation where the plates were forced together and a pressure was applied.

8.3.1 Model

The model was a cut out of two plates in the same way as in the design exploration simulations and as seen in Figure 7.7. Instead of modulate the plate in CAD the tools were modulated as seen in Figure 8.2.

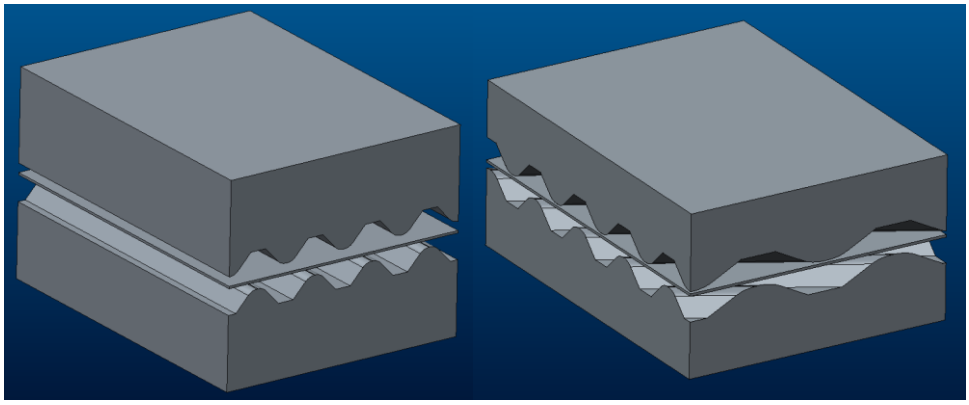

Figure 8.2. Forming tools for both top and bottom plate

8.3.2 Material Model

The material model used in the forming and pressure simulations differed slightly from the model used in the design space exploration simulations. It was based on Barlat and Lean's material theory [6] and the most important difference was that anisotropy was adopted. The plastic strain/stress curve was in principal the same although it contained more data points than the model used in the design

exploration simulations. The two material models can be seen in Figure 8.3. The theory about the anisotropic material model can be found in the theory chapter.

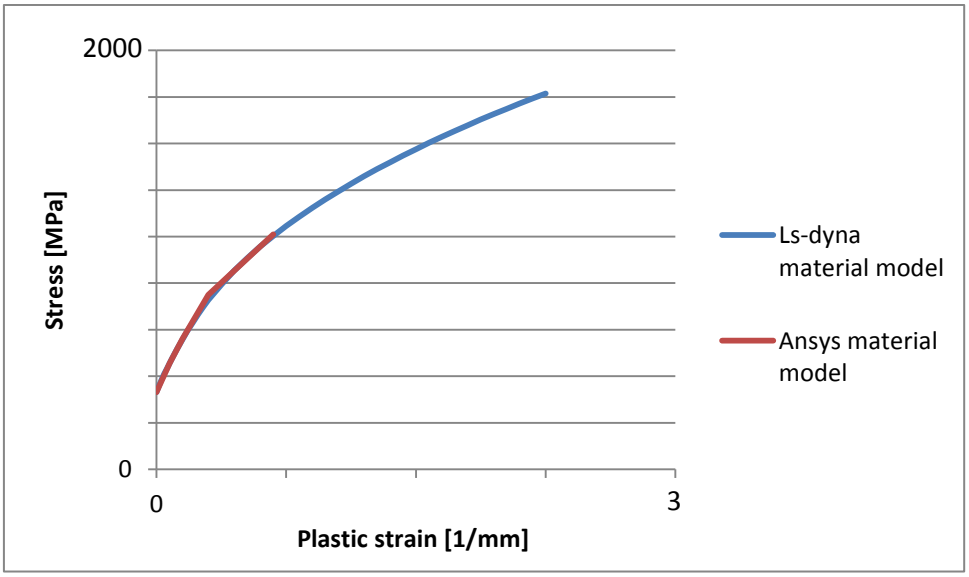

Figure 8.3. Comparison of material models

8.3.3 Boundary Conditions

In the forming simulations the plate edges were constrained, not being able to move in the normal direction to themselves. The friction between the tool and plate was set to a value which Alfa Laval uses when simulating lubricated forming processes.

In the pressure simulations the plate edges were locked to each other in z-direction, normal to the flat surface of the plate. This means that the nodes could move in z-direction but all nodes at the boundary were forced to move equally. This was made to make sure the plate was not bended by the pressure in the unsupported edges.

8.3.4 Mesh

The mesh size was chosen with Alfa Laval's guidelines. The formed plate was meshed with size 0.4 mm. The tool parts were meshed with a mesh size varying between 4 mm and 0.01mm.

8.3.5 Forming Simulation

The geometries were imported from Creo to Dynaform where the model was set up. The geometries i.e. die, stamp and plate were imported as surfaces in IGES files. Figure 8.4 shows the setup in Dynaform with the green stamp, the red die and the blue plate in between. In Dynaform meshes, boundary conditions, stamp motion etc. were applied. The stamp was forced to a specific distance and not controlled by an applied force to form the plate. When the simulation was correctly set up, a Dyn-file was created. The correct material properties were adjusted before it was sent to the solver LS-dyna. The outcome from the solver was a Dynain file containing the formed plate with all information about internal stresses, thickness reduction etc.

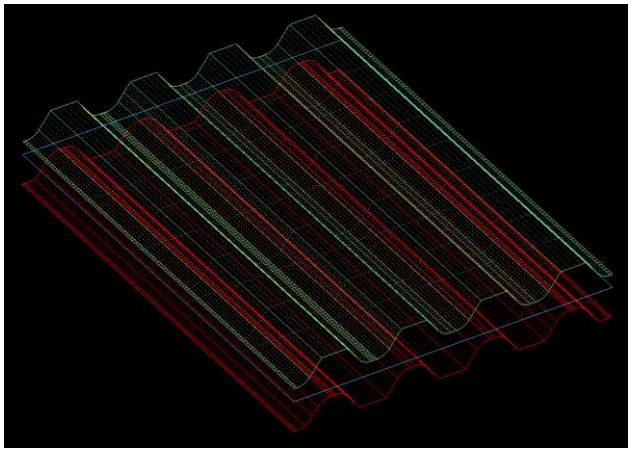

Figure 8.4. Geometries in Dynaform

8.3.6 Pressure Simulation

From the forming simulations the plates were imported as Dynain files to Dynaform. To make sure node, element and part numbers would not collide with each other they were manually changed in LS-prepost for the second plate. Except from the two simulated plates two flat surfaces were imported, meshed and positioned at each side of the two plates. The purpose with the two flat surfaces was to force the plates together as done when the heat exchanger is mounted. The simulation set up can be seen in Figure 8.5 and Figure 8.6.

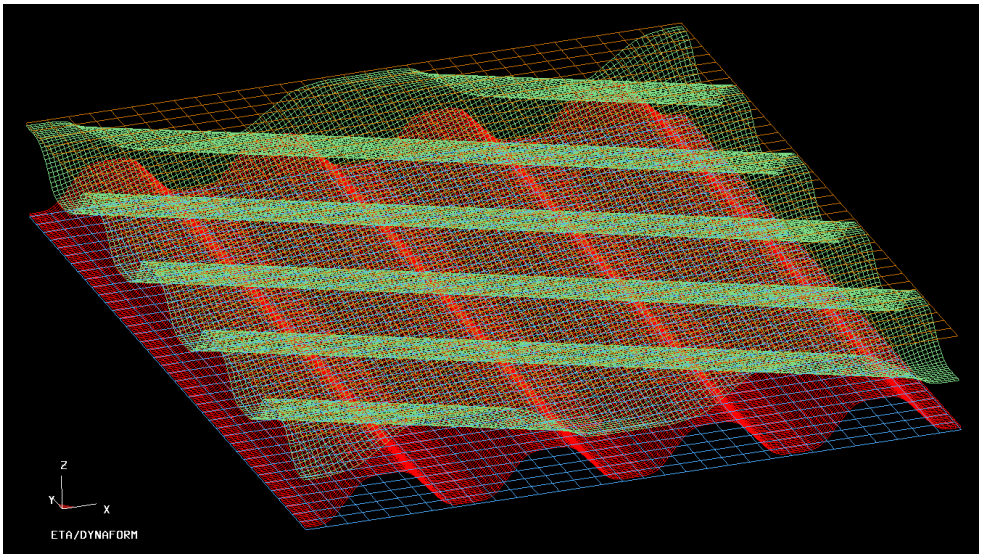

Figure 8.5. Pressure simulation model setup

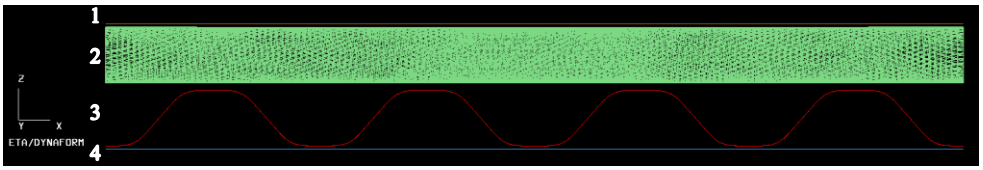

Figure 8.6. Model setup, sideview. 1 Rigid plate, 2 Top plate, 3 Bottom plate, 4 Rigid plate.

Ls-dyna files were created when the plates were correctly set up in Dynaform. The both Dynain files (the plates) from the forming simulation were opened in Ls-prepost and the boundary conditions were applied. An already written dyn file, which Alfa Laval always uses for pressure simulations was copied and modified with information such as times steps, how much the plates should be forced together, the load curve and which geometry files that should be included in the simulation. The load was ramped up to maximum half way through the simulation and ramped down to zero again during the second half. The dyn file was then solved with LS-dyna. As described above several steps had to be manually controlled in the forming and pressure simulations.

8.4 Post Process of Results

8.4.1 Measurement

The deformation results on the plates were measured in a different way than in the design exploration simulations. An area around the interesting point was selected and the maximum and minimum value was displayed as seen in Figure 8.8. The value of interest was documented in an Excel arc where all data were collected. All of the summarized results can be found in chapter 10. Figure 8.7 shows the bottom plate after a forming and pressure simulation.

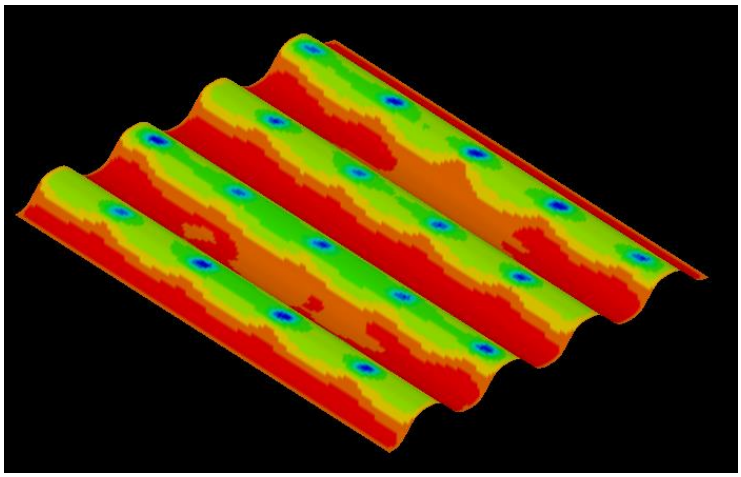

Figure 8.7. Z-deformation (normal to the undeformed plate) is displayed

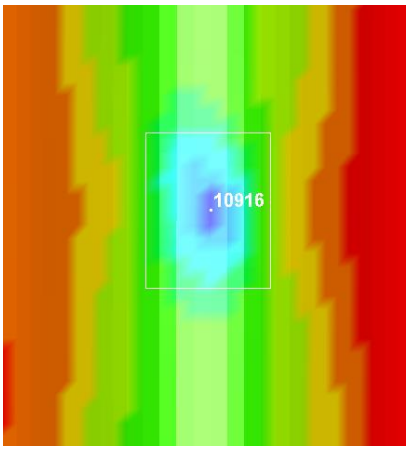

Figure 8.8. A contact point with the node with minimum value marked.

9 Laboratory Experiments

To know if the simulated models were realistic and reliable they were verified by examining the reference plate. A description how it was made by laboratory experiments follows.

9.1 Constraints

Two different plate thicknesses were tested, 0.4 mm and 0.5 mm, to make sure that the models were independent of the plate thickness. The experiments were limited to four pressure levels for each plate thickness, i.e. totally eight tests were performed. An attempt to measure the global deformations was made but since it was difficult to measure them with a satisfying accuracy they were not included in the analysis. Instead only the local deformations were analyzed.

9.2 Experimental Approach

Different pressure levels were applied and the deformations were examined at each level. After a test with a certain pressure had been run the plates were replaced with new plates for next pressure level. The first test of each plate thickness was first assembled with an extra plate which was taken out before the pressurization. These extra plates were references to see if any deformations occurred due to the forces from the assembly process.

9.2.1 Pressure Levels

Different pressures were used in the tests to make sure that the simulations follow the reality through all time/pressure steps. It was important to make sure the tested pressures gave remaining deformations. To decide which pressures to use the maximum allowed test pressure was tried first. Note that the maximum allowed test pressure is decided with safety factors, which means that the proved actual leakage pressure is higher. After the first tests the PHE was disassembled and the plates were examined ocularly. The deformations were considered to be moderate,

i.e. they were visible but it was estimated that they were far from fracture. With this in mind the rest of the pressure levels were chosen. Since the deformations were considered moderate one test level with lower pressure and two with higher were used. The plastic strain curve is not linear; hence, it is important to have smaller steps between the higher pressures than the lower. The pressures in Table 3 were chosen as the test levels.

Table 3. Pressure levels at tests*

Pressure Levels (barg)	Plate thickness 0.4 mm	Plate thickness 0.5 mm
Max. design pressure	$p_{1,0.4\,mm}$	$p_{1,0.5\,mm}$
Max. test pressure	$p_{2,0.4\,mm}$	$p_{2,0.5\,mm}$
In between	$p_{3,0.4\,mm}$	$p_{3,0.5\,mm}$
A few bars below leakage pressure	$p_{4,0.4\,mm}$	$p_{4,0.5\,mm}$

Explanation of pressures limited by plate:

- Maximum design pressure – The maximum pressure that can be used during operation.
- Maximum test pressure – The maximum pressure the PHE can be tested with after assembly
- Leakage pressure – The maximum proved pressure obtained in laboratory before the PHE starts to leak.

9.2.2 Material

Material certificates were obtained from the sheet material manufacture with tested material properties. Different material batches were used for the 0.4 mm and 0.5 mm plate thicknesses. Relevant data from the material certificates are seen in Table 4.

Table 4. Material properties at room temperature

Plate thickness	Yield Strength (Rp0.2%)	Tensile Strength
0.4 mm	290 MPa	604 MPa
0.5 mm	281 MPa	581 MPa

* Confidential Alfa Laval information

9.2.3 Measurement

After all plate packages had been pressurized they were sent to the material laboratory at Alfa Laval in Lund to be measured with blue laser. The middle plate of each plate package was picked out and a sample was cut out of each plate, as seen in Figure 9.1.

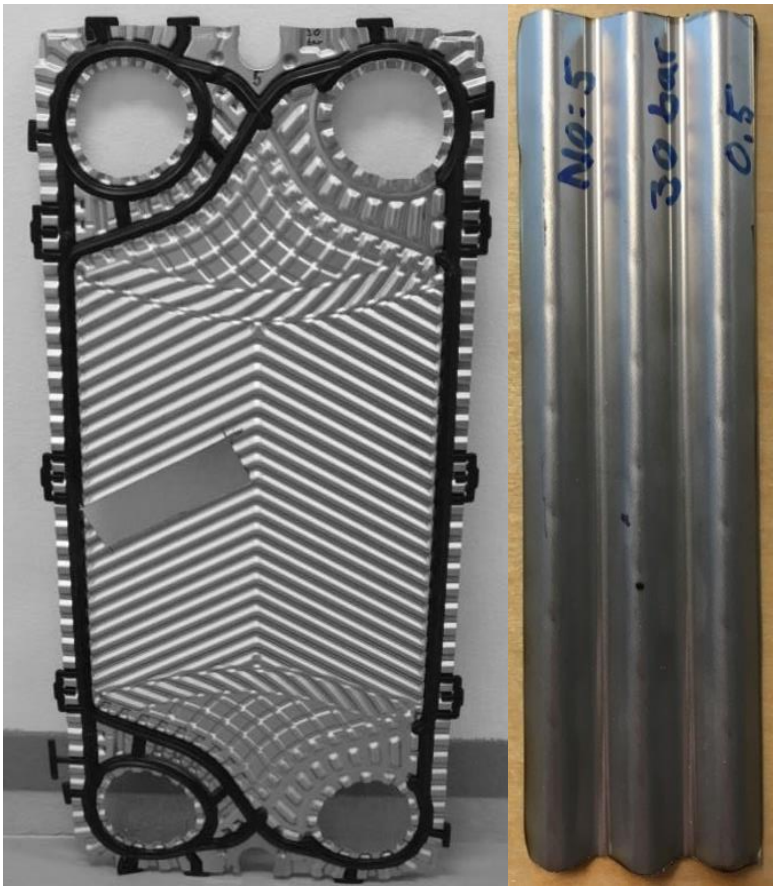

Figure 9.1. Plate with sample cut out and a sample of 0.5 mm plate pressurized to $p_{4,0.5\,mm}$ barg

The measurement was performed with blue laser equipment from Keyence. It had an effect of 4.8 mW and a wavelength of 405 nm. The samples were manually put in the right position under the laser and an attempt to measure both the local and global deformations was made, see Figure 9.2 and Figure 9.3.

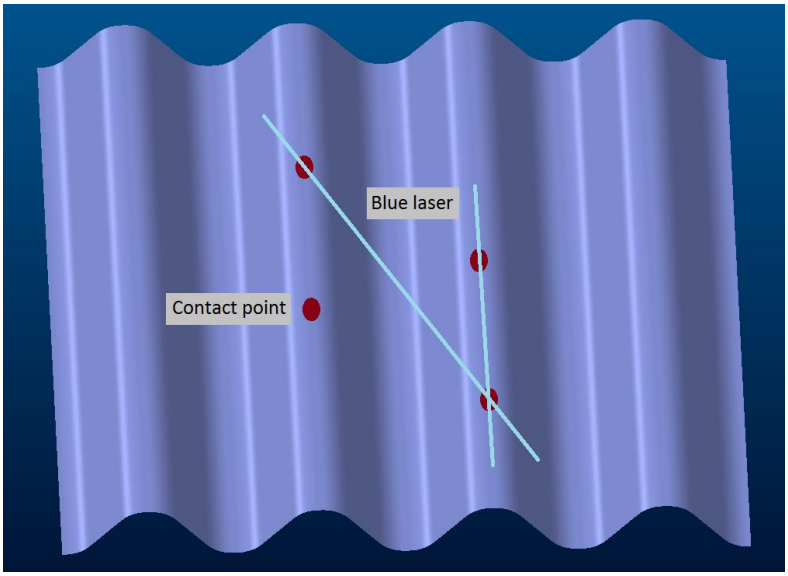

Figure 9.2. Measurement with blue laser

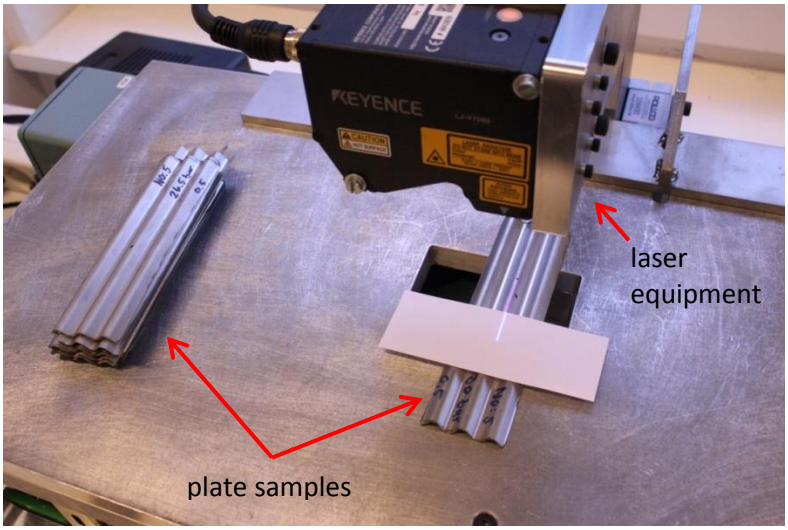

Figure 9.3. Measurement with blue laser

9.2.4 Post Processing of Results

The obtained data from the laboratory experiments had to be processed before it could be interpreted. As seen in Figure 9.4 the plate was not placed in a completely flat position and the data therefore had to be compensated. In Figure 9.5 the inclination between the two minima has been measured and a linear curve coefficient has been added. In Figure 9.6 the maximum between the two minima

has been moved to zero at the y-axis. It was not perfectly clear which level between the two minima that represented the real plate surface. The maximum could be caused by reflections, dust etc. but the maximum was a point which was easy to define. Therefore, it was chosen as the reference point. When evaluating the results it was important to keep in mind that the noise was a source of uncertainty.

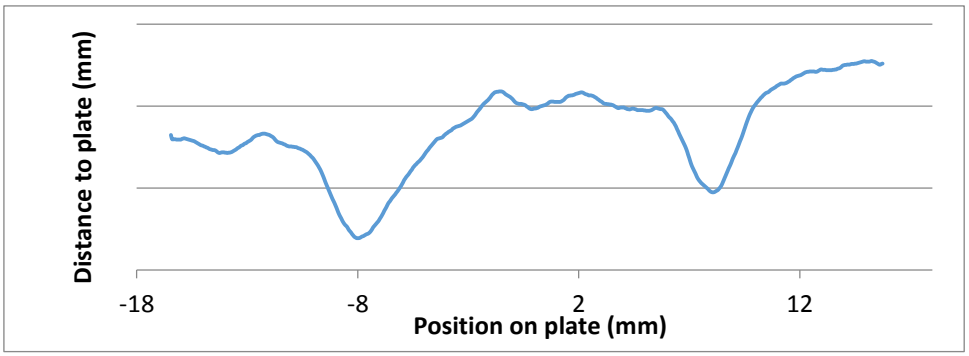

Figure 9.4. Raw data from laboratory experiments

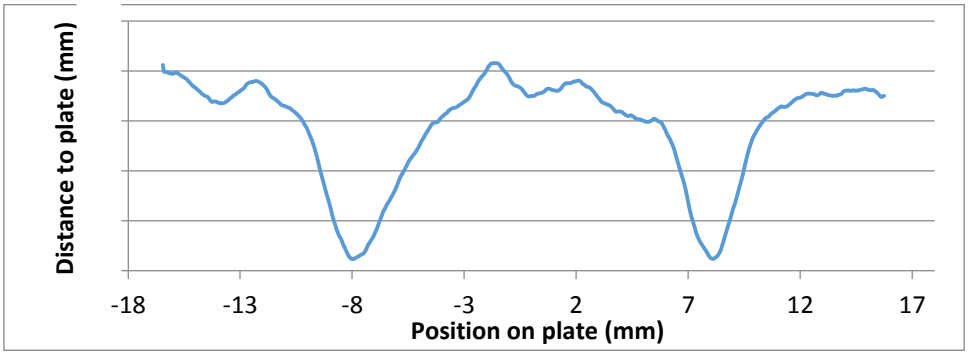

Figure 9.5. Modified raw data

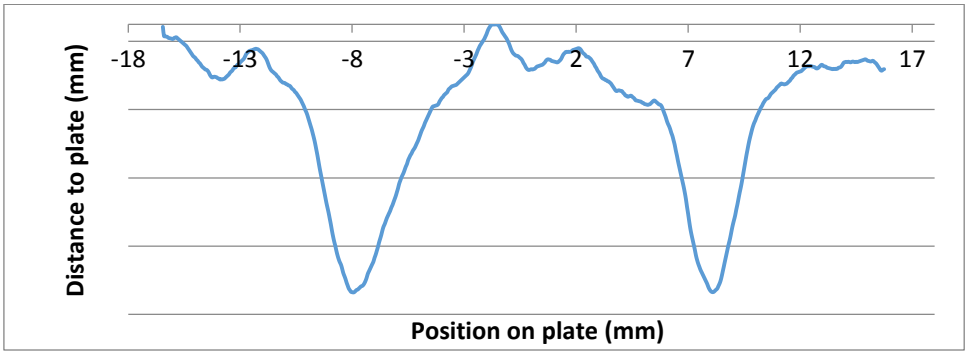

Figure 9.6. Modified raw data

As seen in Figure 9.7 the data series needed to be horizontally offset to make them easier to compare. In Figure 9.8 the left hand minima have been modified horizontally to fit over each other.

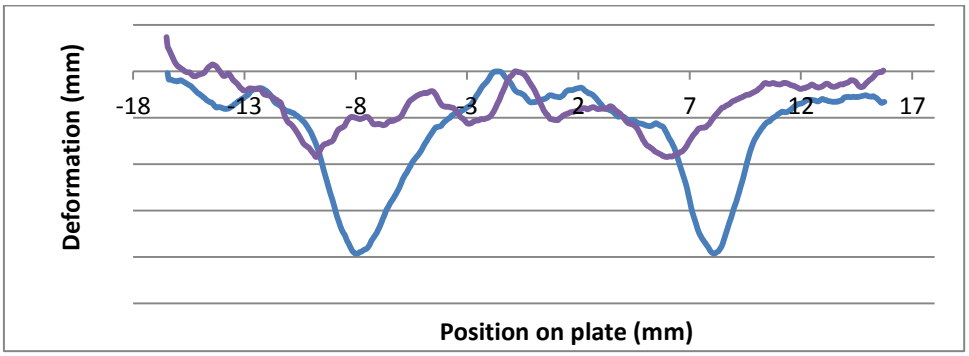

Figure 9.7. Data without horizontal offset

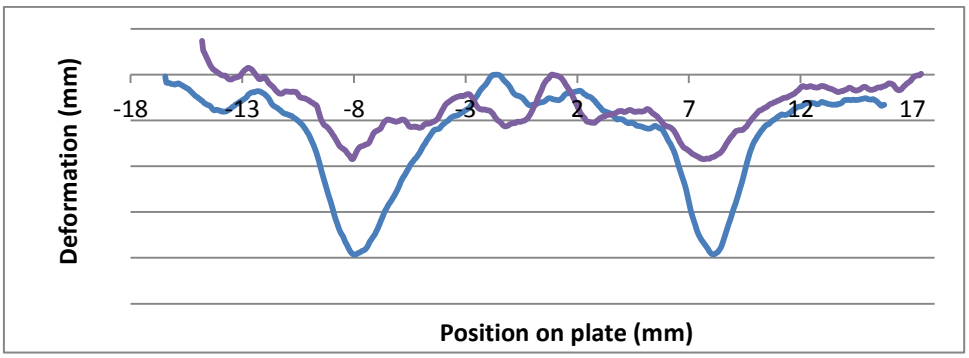

Figure 9.8. Data series with horizontal offset to each other

10 Results

All the results are shown in this chapter. First each section is displayed separately and finally the results are compared to each other.

10.1 Design Space Exploration

The results are analyzed and discussed in chapter 11.

10.1.1 Initial Design Space Exploration

The results from the design space exploration shown in Figure 7.1 are displayed in Figure 10.1 to Figure 10.3. Figure 10.1 shows how the deformation differed over the varying angles and shows both global and local deformations.

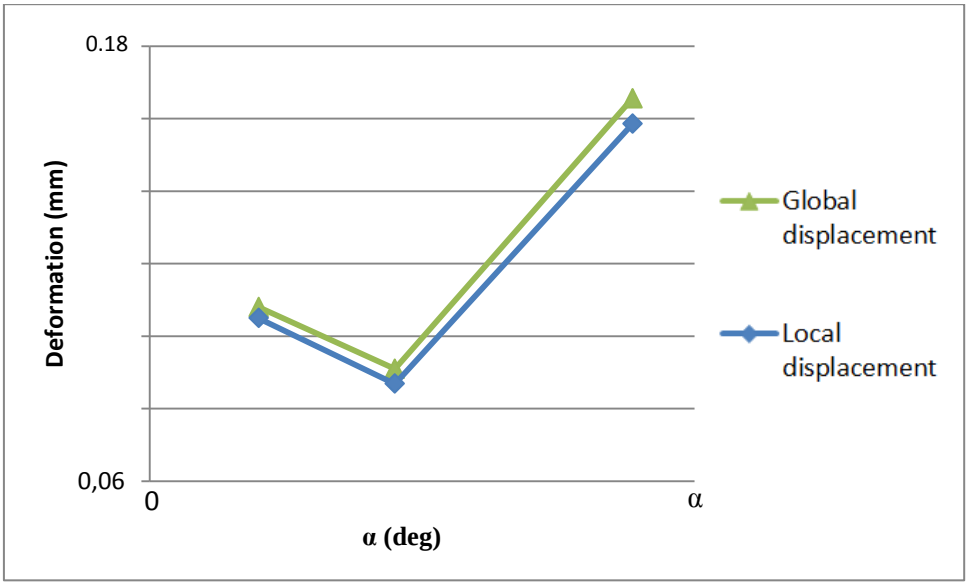

Figure 10.1. Comparison of global and local deformation. Bottom plate, r_1

Figure 10.2 shows how the deformation differed over the varying radius for different angles. Figure 10.3 shows how the deformation differs over a varying angle for different radiuses. Both figures show average values between top and bottom plates.

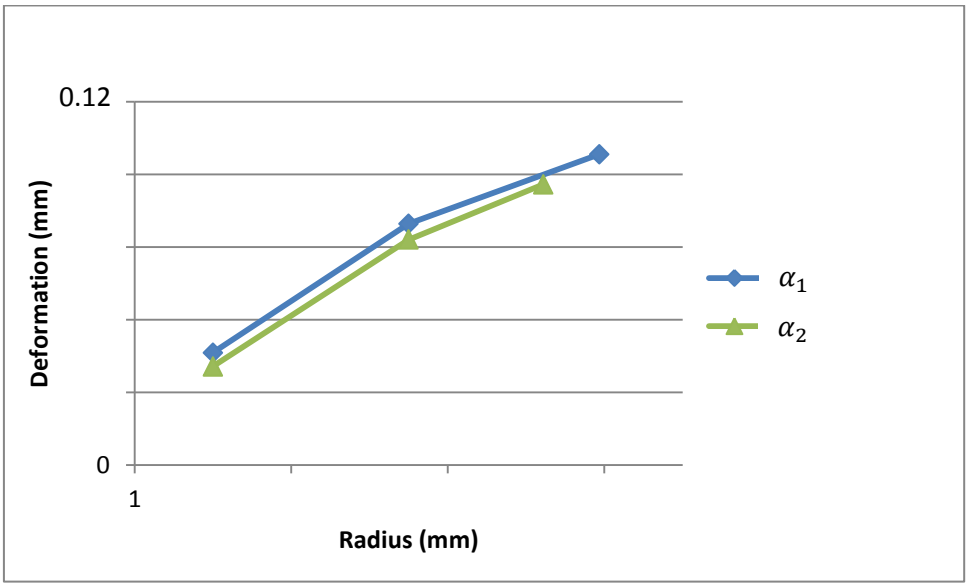

Figure 10.2. Results of the design space exploration

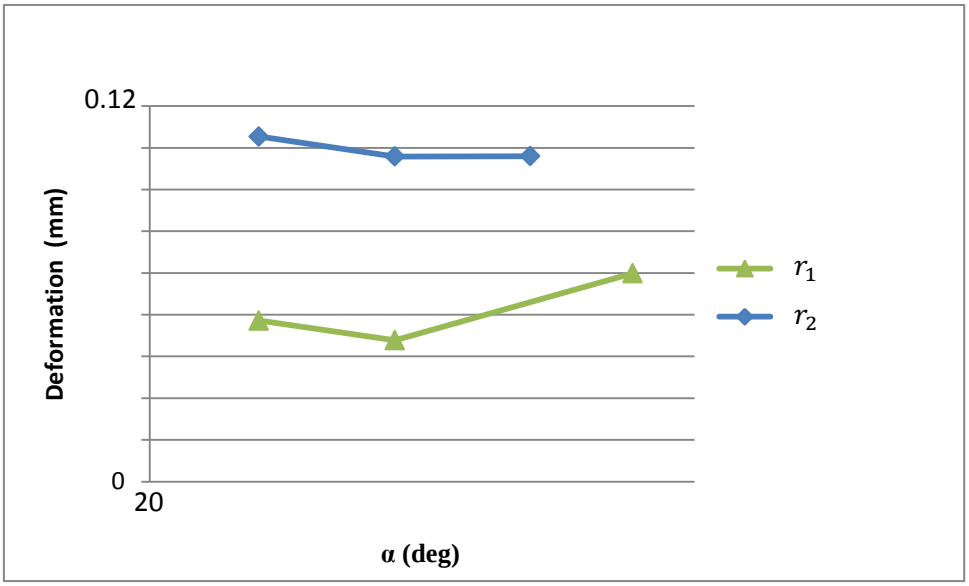

Figure 10.3. Results of the design space exploration

10.1.2 Zoomed in Study

Figure 10.4 shows different radiuses with a varying angle. The values are the average between top and bottom plate.

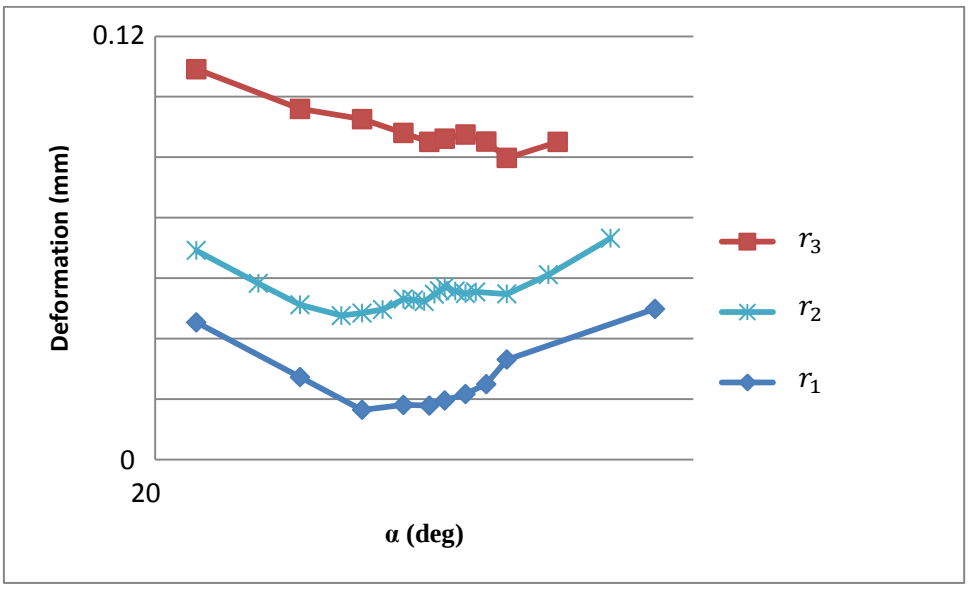

Figure 10.4. Simulations at three different radiuses

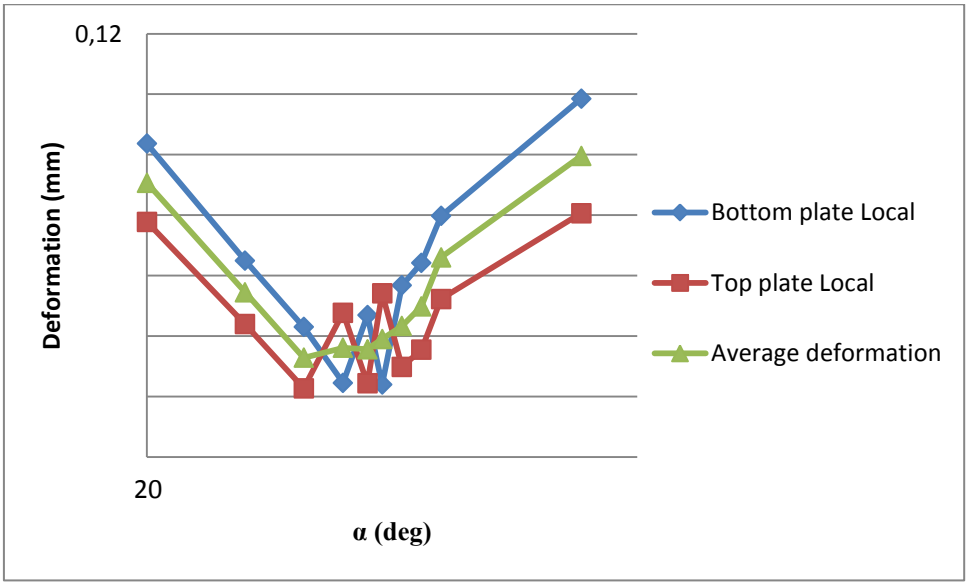

Figure 10.5. Radius = r_1

10.2 Forming and Pressure Simulations

Only the local deformations were evaluated and an average value of the top and bottom plate where calculated as shown in Figure 10.6 and Figure 10.8. The difference between the theoretical and true angle is shown in the figures but can also be seen in appendix.

By mistake the radius was initially miscalculated. The radius was originally defined to the centerline of the plate. In the forming simulations it was initially defined as the tool radius which gave a plate radius of half a plate thickness thicker than expected. This is why radius $r_2 + 0.25$ mm and $r_3 + 0.25$ mm were simulated instead of r_2 and r_3 mm. The simulation with radius r_3 mm was made as a complement.

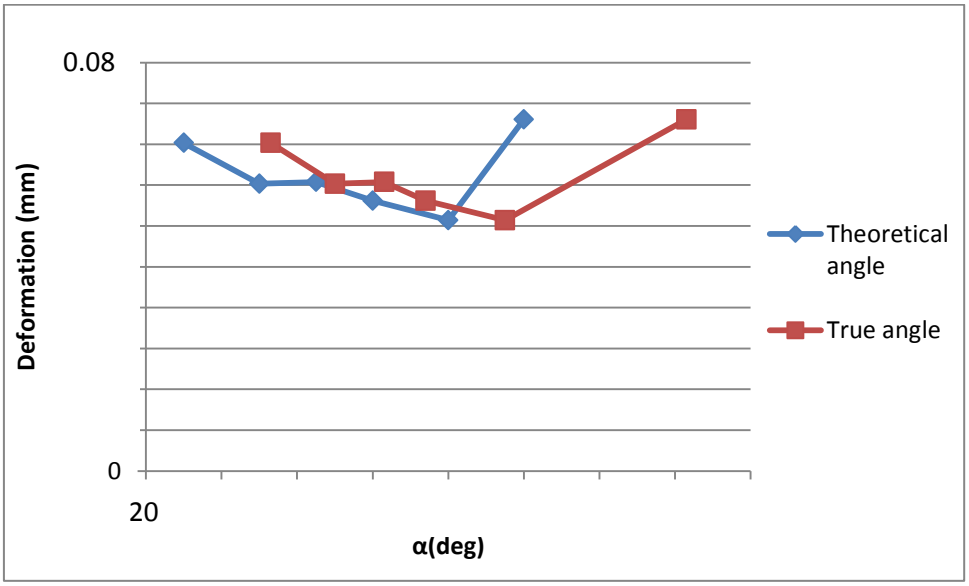

Figure 10.6. Radius $r_2 + 0.25\ mm$. Average of top and bottom plate local deformation

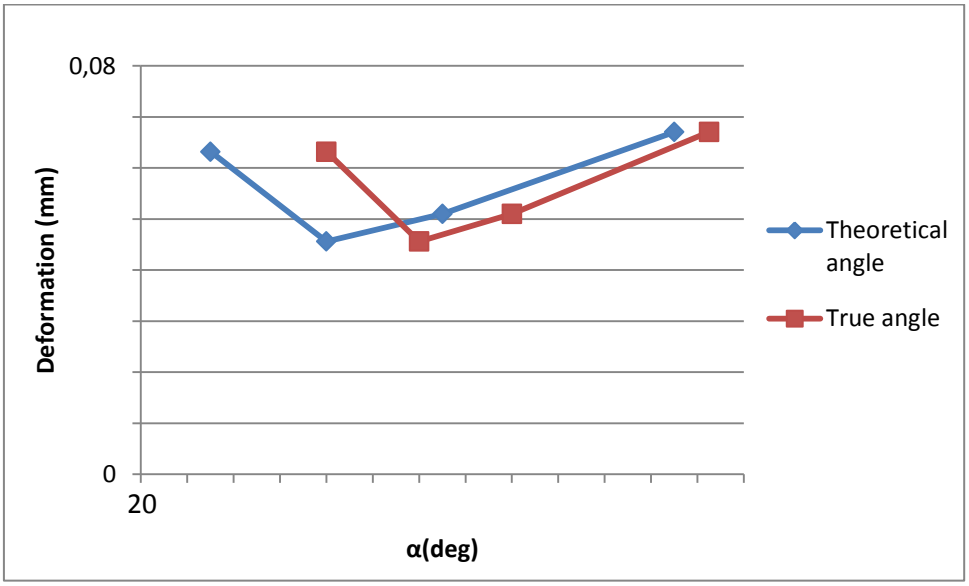

Figure 10.7. Radius r_3. Average of top and bottom plate local deformation

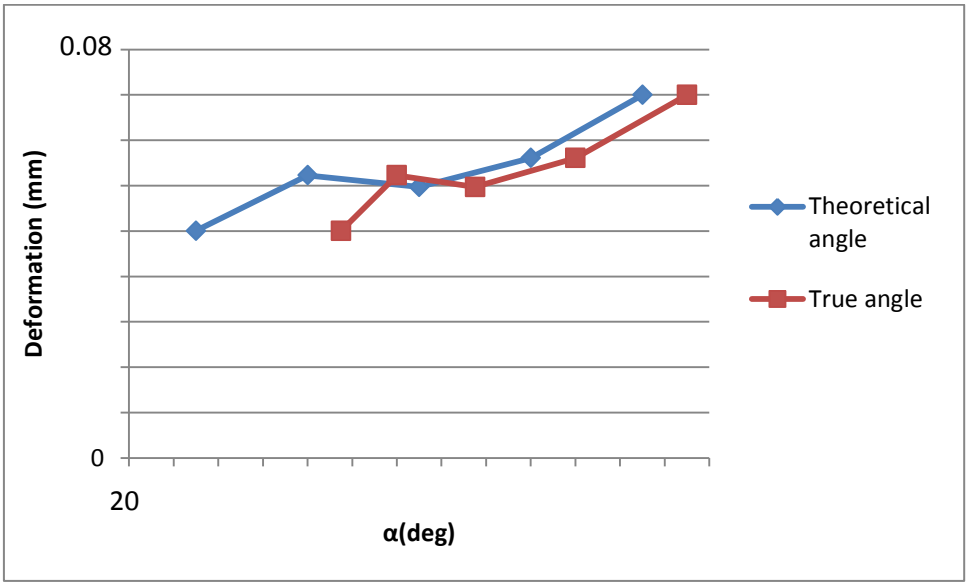

Figure 10.8. Radius $r_3 + 0.25\ mm$. Average of top and bottom plate local deformation

Figure 10.9 shows all forming and pressure simulation results together.

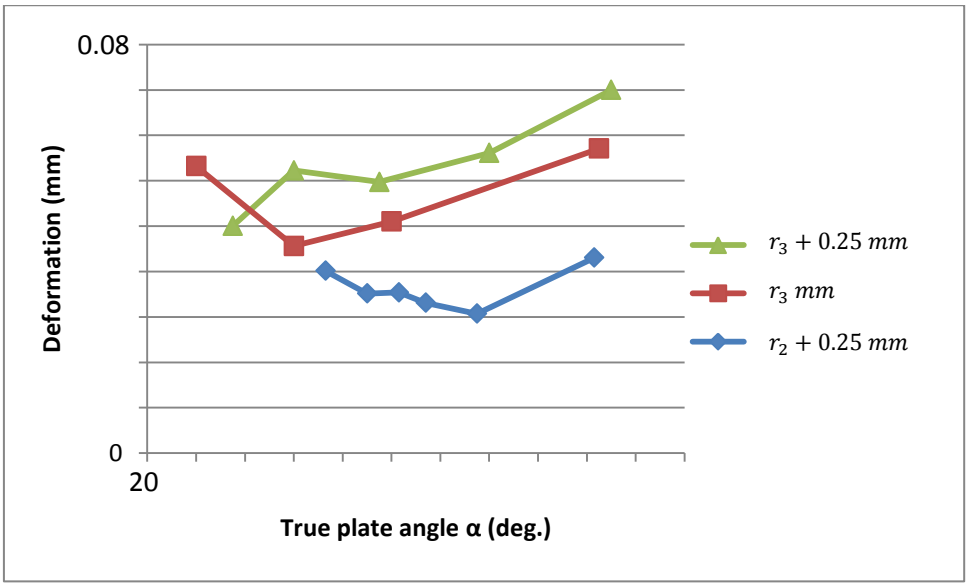

Figure 10.9. Forming and pressure simulations results

Figure 10.10 and Figure 10.11 show the deformation behavior of two different plate angles.

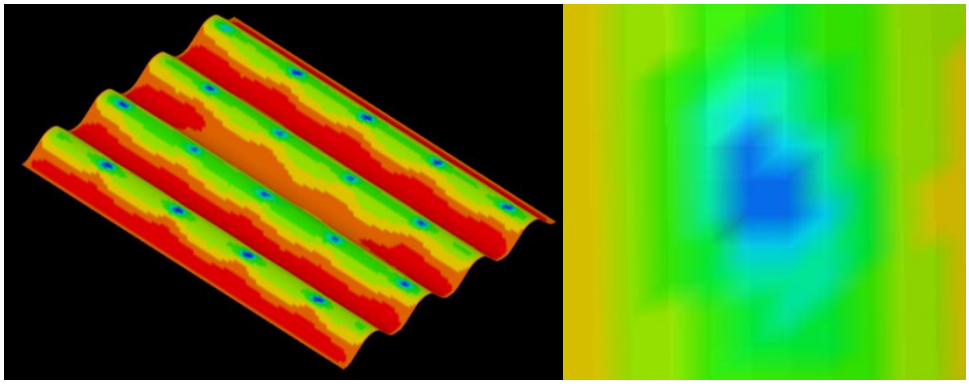

Figure 10.10. Radius r_3

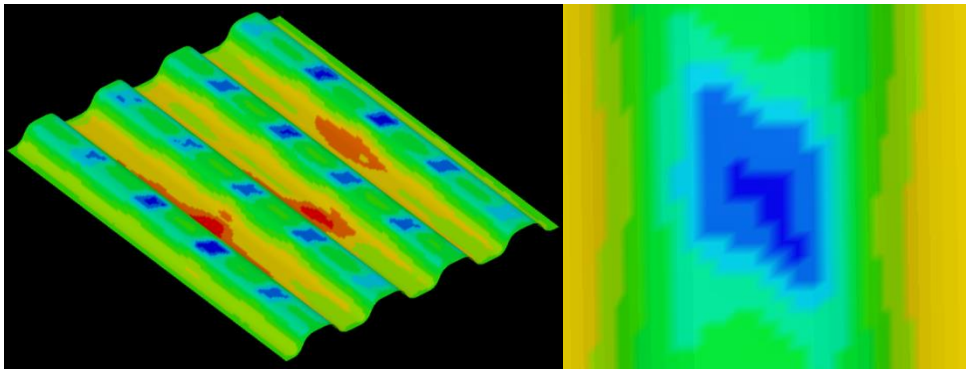

Figure 10.11. Radius r_3

Figure 10.12 and Figure 10.13 show the plate thickness after forming simulation for the top and bottom plate. The scales are the same in both figures. The sheet metal used had an original thickness of 0.5 mm.

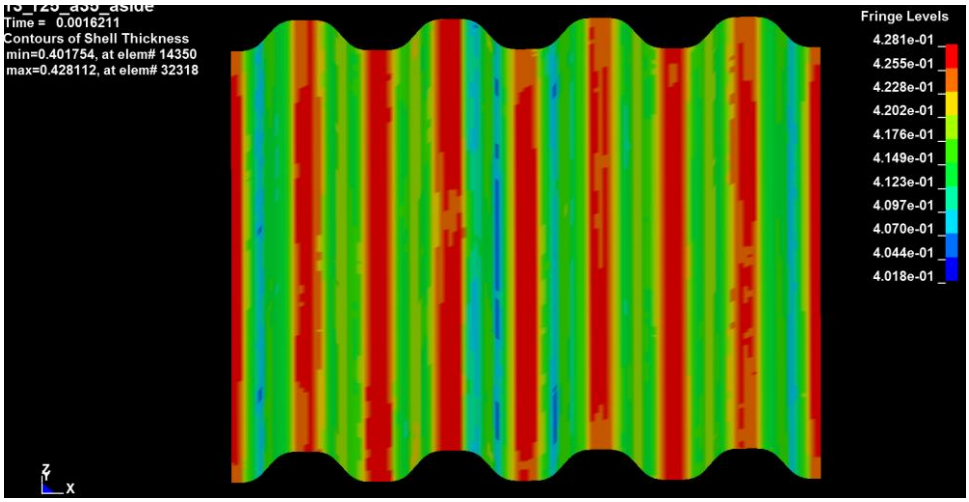

Figure 10.12. Plate thickness after forming (mm), bottom plate, design point 3

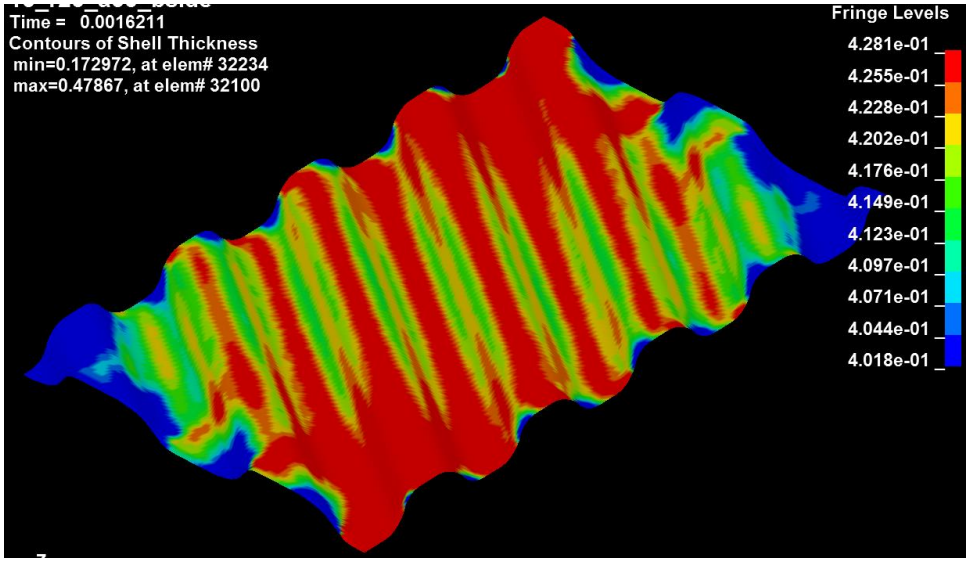

Figure 10.13. Plate thickness after forming (mm), top plate, design point 3

10.3 Comparison of Design Optimization Results

The results of the simulations from both Ansys and Ls-dyna are compared to each other in Figure 10.14 to Figure 10.16.

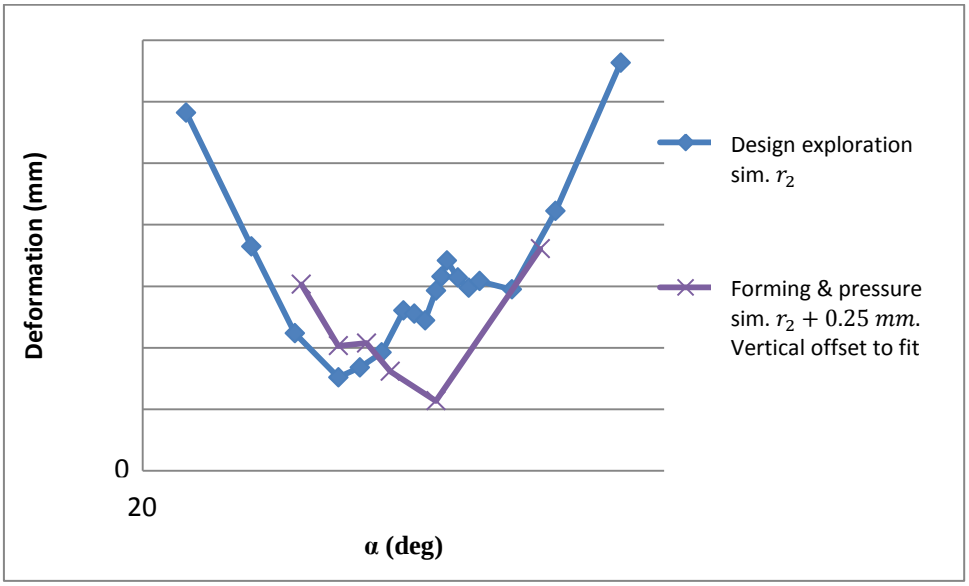

Figure 10.14. Local deformation.

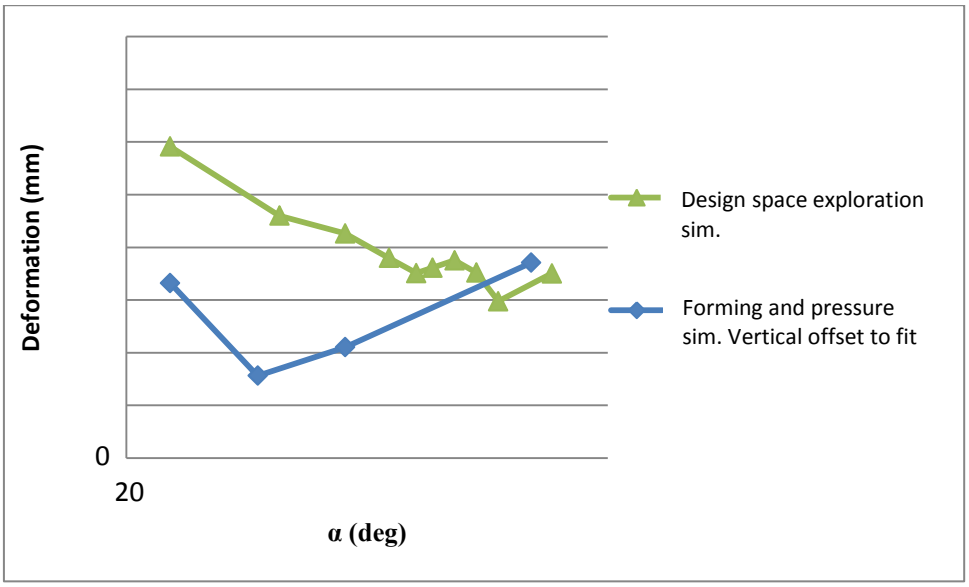

Figure 10.15. Radius r_3. Local deformation.

Since the scale was considered as confidential information three angles, $\alpha_1, \alpha_2, \alpha_3$, were defined in order to be able to discuss the results.

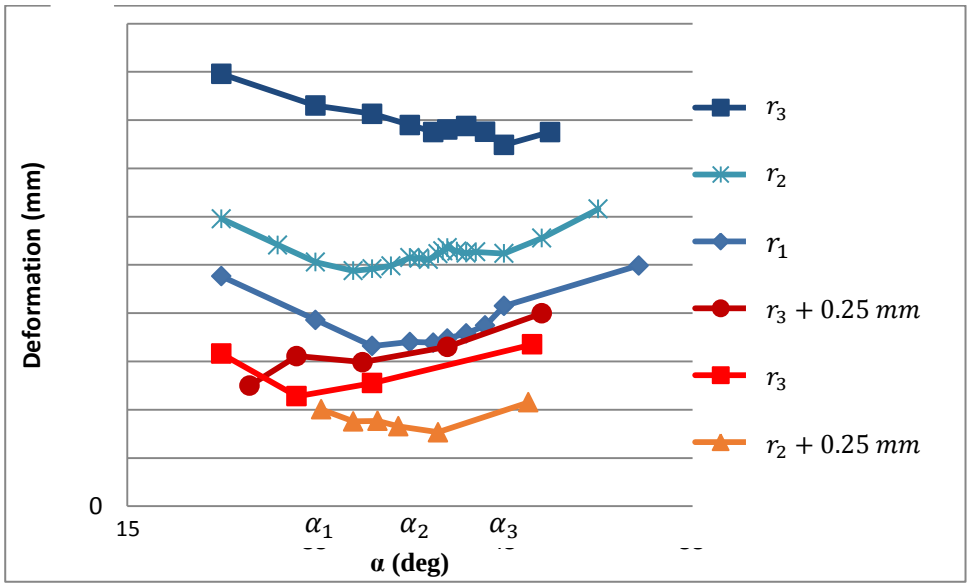

Figure 10.16. Blue curves are design space exploration simulations and red/orange curves are forming and pressure simulations

10.4 Laboratory Experiments

The reference plates which were only assembled and not pressurized had no measurable deformations. Results shown in Figure 10.17 and Figure 10.18 are processed as described in the method.

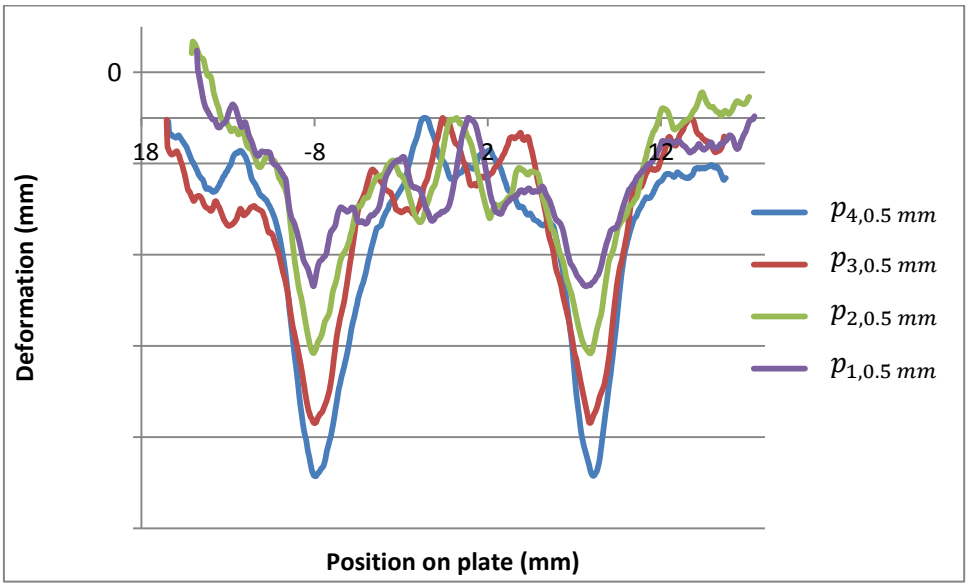

Figure 10.17. Experiment results, the reference plate 0.5 mm plate thickness, 316 stainless steel

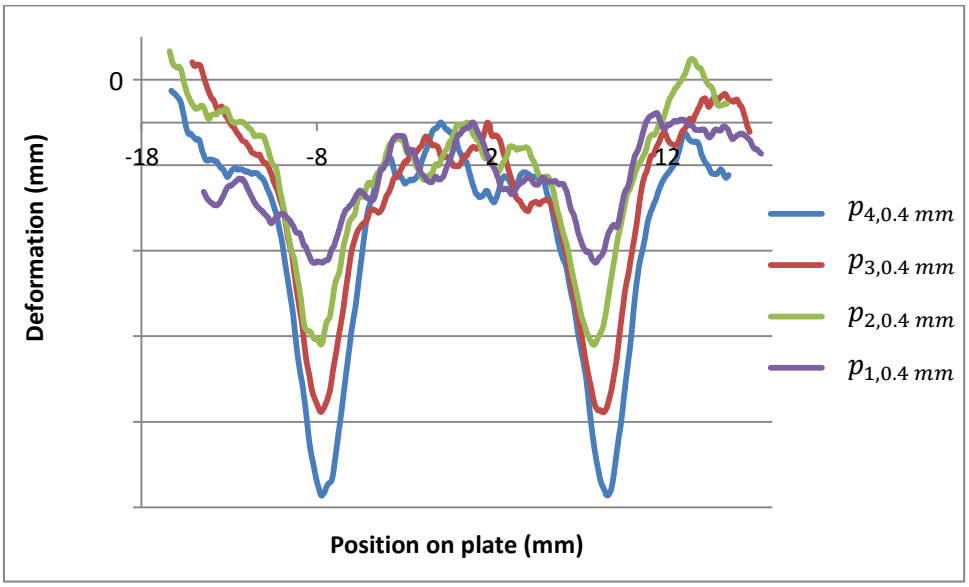

Figure 10.18 Experiment results, the reference plate 0.4 mm plate thickness, 316 stainless steel.

10.5 Verification of Simulation Models

A comparison of the results from the different simulation methods and the laboratory experiments is seen in Figure 10.19 and Figure 10.20. Average values of the top and bottom plate for the simulations are shown.

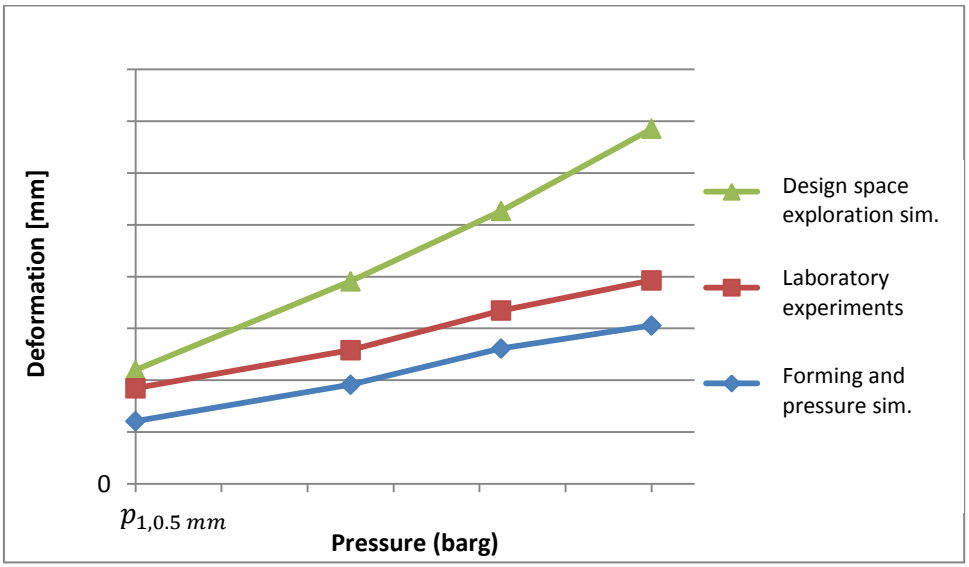

Figure 10.19. The reference plate 0.5 mm plate thickness, 316 stainless steel

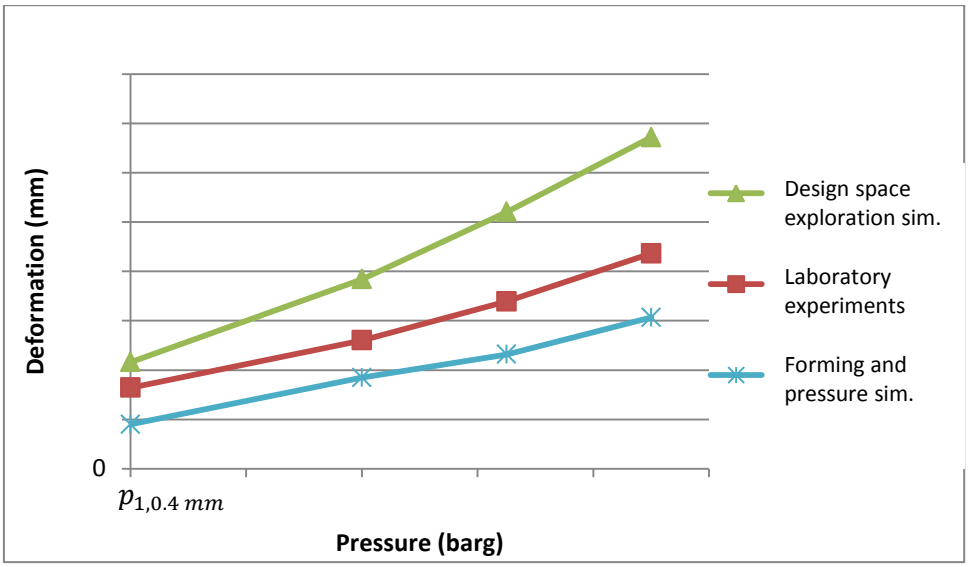

Figure 10.20. The reference plate 0.4 mm plate thickness, 316 stainless steel

11 Discussion

The following chapter discusses the results and which improvements that could have been made. The conclusions of the thesis are also gathered.

11.1 Design Exploration Simulations

The aim of the design exploration simulation model was not to get perfect results but to get a brief picture of the design space. It was already known that the simplifications were considerable and that it would make the result differ significantly from the reality. The expectations were rather to see if any geometry dependencies could be found and if these trends, despite their absolute values, would correspond to more precise calculation models or to reality. It was considerably easier to run a large amount of simulations with this model than the forming and pressure simulation model, which was a great benefit.

Two obvious effects as a result of the neglected forming procedure were identified. When a plate is formed it becomes thinner, but not homogenously thinner as it was modulated in this model. The thinning occurs more locally as seen in Figure 10.12 and Figure 10.13. The inhomogeneous thickness affect should have an impact on the results, but it was not completely clear if the affect should make the deformations greater or smaller. Another aspect which was not considered is the hardening of the metal which occurs when the plates are cold formed. The hardening affect should have made the deformations smaller if they were considered.

It is seen in Figure 10.1 that the differences between global and local deformations were next to none. This was seen in all of the design exploration simulations. Yet, the global deformations were slightly greater than the local deformations, which indicate that there might occur more deformations than just the local ones. Since it looks like the local deformation accounts for the major part of the deformation together with the fact that it was hard to measure the global deformation properly, the global deformations were not included in the further analysis. An investigation about the impact of the global deformation has been noted as a possible future improvement. The effect from the unevenly distributed plate thinning may increase or decrease the difference between global and local deformation.

Figure 10.5 shows the local deformation for top and bottom plate with a r_1 radius. It can be seen that there is a difference between top and bottom plate and that there are notches on the two curves. It seems like the values between top and bottom plate for some design points have changed places. Though the reason for this is not clear, it is probably caused by unidentified of instabilities in the model. When an average of top and bottom plate was calculated the resultant curve looked more correct, which can be seen in Figure 10.4. One contributing reason for this can be that the top plate was constrained in each corner unlike the bottom plate. Another reason can be the way the upper plate was cut in an angle with a different boundary compared to the bottom plate. However, as long as the two plates show the same trend, the vertical offset in the figure is a minor problem.

11.2 Forming and Pressure Simulations

The anisotropic material model was directly adopted from Alfa Laval's forming and pressure simulation procedure. The direction of the material was not adjusted to fit the model which has been a source of error, although it was considered to be of minor importance since stainless steel is an isotropic material unlike e.g. titanium. It may have contributed to the difference between upper and lower plate since they were oriented differently in relation to the material model. This is something that can be improved, to gain better control over the directions of the material. Despite this the results show that the simulation model corresponds well to the experimental results so the ignorance of the material directions was accepted.

The plate thickness after the forming simulations, which is shown in Figure 10.12 and Figure 10.13, reflects that the top and bottom plate differed slightly from each other. The overall magnitude of the plate thickness was virtually the same for both plates, which was the most important aspect, but although there was still a difference. It is probable that the difference partly was caused by the different cut out orientations of the sample plates. This may have contributed to the difference in deformation between the two plates. A larger simulation model could have made this error smaller.

When the tools were designed a theoretical plate angle was calculated. As expected, it was seen that the theoretical and measured plate angle (i.e. true angle) differed from each other. When the plate becomes thinner the radius, which is measured from the middle line of the plate, also becomes slightly smaller. This causes an uncertainty of the relation between plate angle and radius of the formed plates and the line elongation might also differ marginally.

One improvement could have been to have done more forming and pressure simulations. There could also have been larger differences between the simulated radiuses. The radiuses differed only 0.75 mm and not over the whole design space.

However, the amount of simulations needed to be limited due to the time limitations of the thesis. The simulations modulated with a radius of $r_2 + 0.25$ mm were supposed to be modulated with a radius of r_2 mm instead. Nevertheless, it was impossible to completely control the radius of the plate since it was affected by uncertainties in the forming process, e.g. plate thinning.

The shapes of the plotted curves in Figure 10.9 differ from each other even though the radiuses are close to each other. This could be an indicator of instabilities of the simulation model. One possible reason can be that the mesh size was too big to reflect the small variations of the radiuses.

An aspect that the forming simulations did not include was the spring back effect of the plate after forming. This may affect the results slightly but was estimated to be negligible.

11.3 Laboratory Experiments

The laboratory experiments gave clear results of the local deformation. An attempt to measure the global deformations was made, but there were too many sources of errors to get any clear results. To measure the global deformations the plate depth had to be known and since it may vary between different plates and eventually even on different places on a plate, it was considered too uncertain. Another source of error occurred when the plates were measured with the laser. When the local deformations were measured the laser was placed along one wave top. When the global deformations were measured, the laser was placed over two contact points as seen in Figure 9.2. It was more difficult to aim at a contact point that was barely visible than to aim along a wave top so the measurement might not have been perfectly made over the contact points.

During the post processing of the results they were modified to be easier to interpret. The samples were not lying completely flat when they were measured and this was compensated with a linear function. When the data was vertically offset a point between the two minima had to be chosen as the zero level i.e. the flat plate surface between two contact points. The minimum and maximum values in this area differed approximately 0.01mm and this was probably caused by reflections on the surface. It was impossible to know where the plate surface truly was. Perhaps an average value could have been more accurate, but to make it simpler the maximum value was chosen. This was, nonetheless, a source of error which had to be taken into account.

11.4 Comparison of Results

11.4.1 Verification of Simulation Models with Experiments

The experimental results were found in between the two simulation models as seen in Figure 10.19 and Figure 10.20. It seems as though the design space exploration simulations exaggerated the deformations and the forming and pressure simulations underestimated the actual results. If the errors that may be caused when the experimental results were offset the actual results could be about 0.01 mm smaller. If that is true, the forming and pressure simulations were close to the reality and the design explorations are even more exaggerated. It can be seen that the design space exploration curve diverges from the other curves at an increasing pressure. This can most likely be explained by the neglected forming procedure. When a plate is cold formed it becomes hardened and the yield limit increases, the forming simulations included that aspect. Since the plastic strain curve is not linear the differences between excluding and including that effect increases with an increasing pressure, i.e. increasing strain. The verification strengthens that the forming and pressure simulation are close to reality and that the design space exploration simulations exaggerates the results.

11.4.2 Design Optimization

The comparison of the simulations in Figure 10.14 strengthens the credibility of the results even though they did not reflect the same radius. There did not seem to be any reasonable explanation to why there should be any major differences between a radius of r_2 mm and $r_2 + 0.25$ mm. The most important aspect to notice is that both curves show that there should be an optimal angle to be found. Figure 10.15 is confusing since the simulation methods indicate different optima. The design exploration simulations indicate that the optimum should be at a higher angle and the forming and pressure simulations indicate that an optimum should be found at a lower angle. The forming and pressure simulation model seems to be more accurate; hence, it is more likely that the optimum should be located at a low angle rather than a high one. The irregular results could be caused by too large mesh elements which simplifies too much.

It is clearer, as seen in Figure 10.4 and Figure 10.9, that a minor radius results in minor deformations. All design points, except one point in Figure 10.9, indicates this. Regardless, that irregular design point deviated from the others and an improvement could be to investigate more design points around and to the left of that point.

11.5 General Improvements

The mesh element size of the simulation models may be too large. The element size was 0.5 mm for the design exploration simulations and 0.4 mm for the forming simulations. This means that there cannot be any flat surfaces smaller than this size and the small radiuses become more rugged. The element size directly affects the solving time, which was why it was not desirable to make it too small either. The mesh size could be the reason why the forming and pressure simulations gave confusing results and not perfect curves. A small change in a parameter might cause a greater change of the mesh geometry because of the mesh size.

A general improvement for both of the simulation models could have been to have made two identical plates and rotate one of them to achieve the angle of the Chevron pattern. This may have decreased the differences in the results between the top and bottom plate.

It would have been favorable if several of the design points could have been manufactured and tested with real experiments. This is a matter of time and cost but would have made the results more reliable. If this would have been made, the deformation could have been measured directly over the plate package to achieve the global deformation.

Instead of measuring the tested plates with the laser, which gives results over one line, it would have been better to 3d-scan them before and after pressurization. It would then have been possible to measure and evaluate the global deformation more easily. It would also have removed the uncertainty of aiming the laser in the correct position.

11.6 Thoughts

In trying to at least partly explain the results a short theory as follows was developed. The distance between the contact points are dependent on the geometry which means that the number of contact points of a certain plate area is varying. When the pressure is applied the plate area per contact point will result in a force which each contact point will have to absorb. This relation may, at least partly, explain why an optimum design can be found.

If the idealized theoretical geometry before it becomes deformed is considered, then it is only the flat surface which is in contact. It was discovered that the deformation behavior made the contact points deform like a bowl, as seen in Figure 7.23, which means there is essentially a circuit in the contact point which absorbs the forces. If the contact point force is divided by the circuit length, from

the idealized contact area, a value of force per length unit of the circuit will be obtained. Since there is a direct connection between force, stress and deformation this value can be seen as an indication of the magnitude of the deformation in the contact point.

The pressurized plate area per contact point which results in a specific contact point force was calculated as shown in Equation 18.

$$A_{pressurized\ area/contact\ point} = \frac{16(e + c + \frac{d}{2})^2}{\sin\gamma} \tag{18}$$

Where γ is a consequence of the Chevron angle θ described in Equation 19.

$$\gamma = 180° - 2\theta \tag{19}$$

The length of the circuit around an idealized, undeformed contact point, is shown in Equation 20 with the geometry shown in Figure 11.1. This contact point behavior is also confirmed by Figure 10.11.

$$l_{contact\ point\ circuit} = 4\frac{2e}{\sin\gamma} = \frac{8e}{\sin\gamma} \tag{20}$$

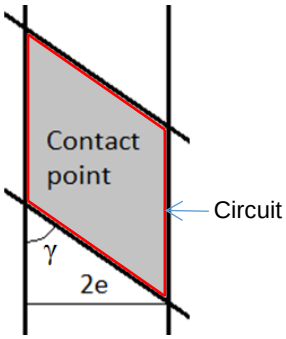

Figure 11.1. Idealized contact point

With an applied pressure of $p_{4,0.5\,mm}$ barg, a line elongation of $\xi = \xi_{com.}$ and a chevron angle of 60° Figure 11.2 is obtained as the correlation of force per length unit as a function of the plate angle. Figure 11.3 shows a zoomed in view of the curve where the radius is close to zero with a clear optimum.

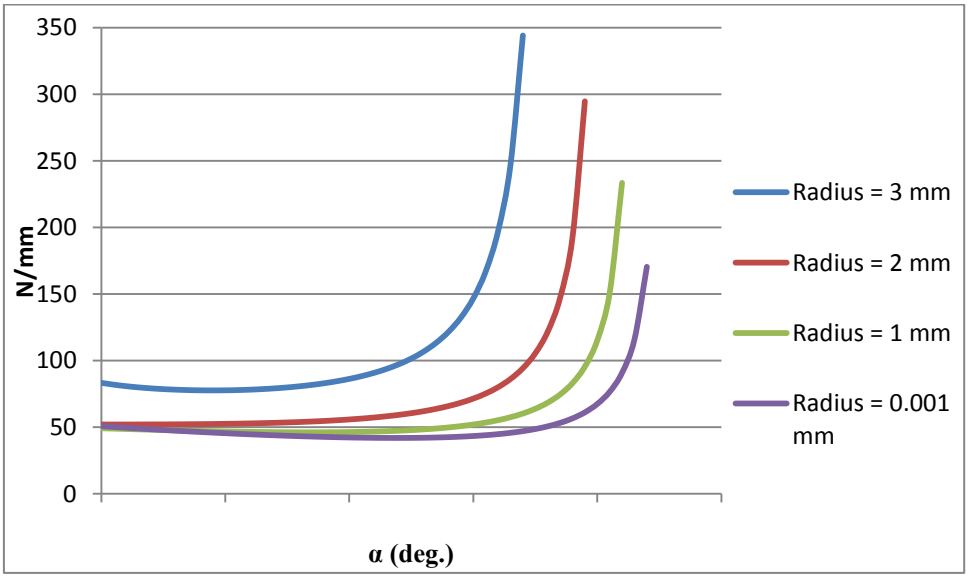

Figure 11.2. Force per length unit of an idealized circuit in each contact point.

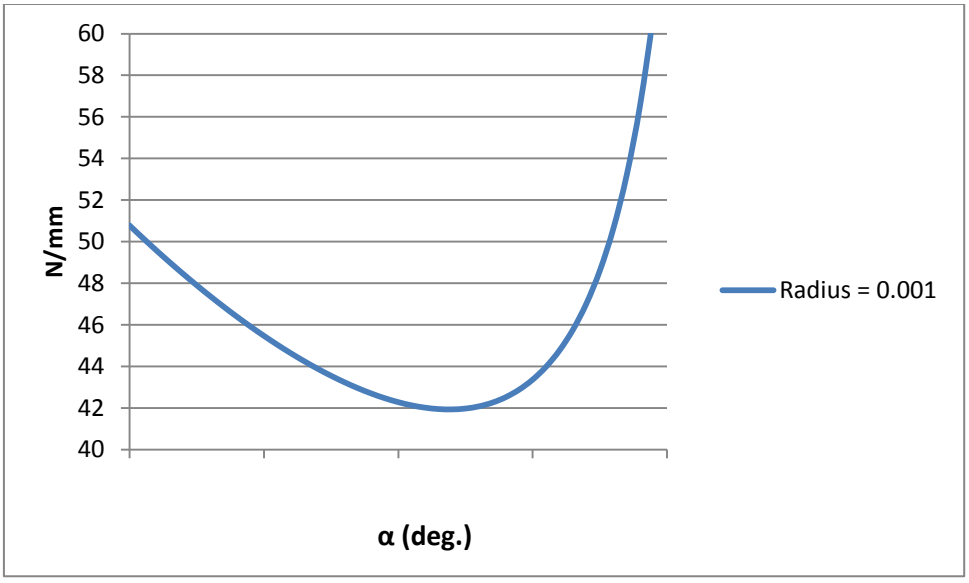

Figure 11.3. Radius close to zero with an optimum angle

This correlation is an idealization and it supposes that the geometry is undeformed, i.e. it corresponds to the initial time step of the pressurization. There are optima for the curves where the radius is 3 mm and 0.001 mm. With a radius of 3 mm there is an optimum at a smaller angle and with a radius of 0.001 mm there is an optimum at a greater angle. The radiuses 1 mm and 2 mm gave no optima in this area.

The reason for the curves turning straight upwards with an increasing angle is that the flat contact surface and the circuit become close to zero. A probable explanation to why the simulation results do not increases this fast is that in reality there is an immediate deformation which increases the contact area and circuit length. If the contact area from the beginning is close to zero a small absolute increase will result in a great relative increase. This means that if a compensation is made for what happens when the deformation has started concerning the points with a greater angle the stress will decrease faster than for the points with a minor angle. If that argument is correct, it could explain why there also are optima for radiuses of r_2 mm and $r_3 + 0.25$ mm and why the real optima are located further to the right (i.e. greater angles) than what can be seen in this theoretical model.

11.7 Conclusions

Regarding the geometry, the conclusion is that the radius should be as small as possible. It is not as easy to give an exact answer about the plate angle. Generally an angle around α_2, seen in Figure 10.16, can be an appropriate target. Angles between α_1 and α_2 can be the optimum. The other parameters must also be evaluated in the choice of design. A mechanically optimized design could be similar to what is shown in Figure 7.2 where the flat surface is relatively large. In a thermal perspective this might not be ideal since the area of the contact points are not directly heat transferring.

Regarding the simulation models the conclusions are that the existing forming and pressure simulations used by Alfa Laval work well and correspond acceptably to reality. The simulations made for the design exploration were relatively far from reality. Nonetheless, it was a useful tool for examining the behavior of the geometry.

It seems likely that the local deformation stands for the major part of the total deformations, but it was only confirmed by the first rough simulation model. It was seen that the global deformations are difficult to measure on a single plate.

11.8 Recommendations for Future Work

One recommendation would be to carry out laboratory experiments in order to investigate the difference between local and global. If the total deformation on a whole plate package is measured and divided by the number of plates, the global deformation for one plate would be obtained. The local deformation for a single plate can then be measured and a comparison can be made.

It would have been interesting to investigate the behavior of titanium plates to see if the material properties have any major impact on the deformation behavior.

Investigating and confirming how the conclusions correspond to different plate depths and plate thicknesses would have been valuable.

Doing laboratory experiments of different plate geometries in the same way as the simulations were done would give a greater credibility to the results of the thesis.

References

[1] Alfa Laval. (2015). Retrieved March 1, 2016, from: http://www.alfalaval.com/.

[2] ASME (American Society of Mechanical Engineers). (2016). Retrieved March 2, 2016, from: https://www.asme.org/shop/certification-and-accreditation/boiler-and-pressure-vessel-certification.

[3] European Comission. (2016). Retrieved March 2, 2016, from: http://ec.europa.eu/growth/sectors/pressure-gas/pressure-equipment/directive/index_en.htm.

[4] Ottosen N, Petersson H. (1992) Introduction to the Finite Element Method. Lund, Sweden: Prentice Hall.

[5] LSTC Inc; Dynamore. Ls-dyna Support. (2016). Retrieved March 11, 2016, from: http://www.dynasupport.com/faq/general/what-are-the-differences-between-implicit-and-explicit.

[6] Barlat F, Lian J. (1989) Plastic behavior and stretchability of sheet metals. Part I: A yield function for orthotropic sheets under plane stress conditions. International Journal of Plasticity.

Appendix A Time Schedule

ID	Task Name	Start	Finish
1	**Planned Schedule**		
2	Initiation and planning	Wed 10/21/15	Fri 10/23/15
3	Cad modulation for design space explorations	Mon 10/26/15	Fri 12/4/15
4	Design space exploration FEM simulations	Mon 11/2/15	Wed 12/23/15
5	Preparation of laboratory experiments	Mon 1/4/16	Fri 1/8/16
6	Laboratory experiments	Mon 1/11/16	Fri 1/15/16
7	Cad modulation for forming simulations	Mon 1/4/16	Fri 2/5/16
8	Forming and pressure simulations	Mon 1/18/16	Fri 2/19/16
9	Completion of report	Fri 2/19/16	Fri 3/18/16
11			
12	**Actual Schedule**		
14	Initiation and planning	Wed 10/21/15	Fri 10/30/15
15	Cad modulation for design space explorations	Mon 10/26/15	Fri 12/11/15
16	Design space exploration FEM simulations	Mon 11/2/15	Wed 12/30/15
17	Preparation of laboratory experiments	Mon 12/14/15	Fri 1/8/16
18	Laboratory experiments	Tue 1/26/16	Fri 2/12/16
19	Cad modulation for forming simulations	Mon 1/4/16	Fri 3/11/16
20	Forming and pressure simulations	Mon 1/18/16	Fri 3/11/16
21	Completion of report	Fri 2/19/16	Fri 4/1/16

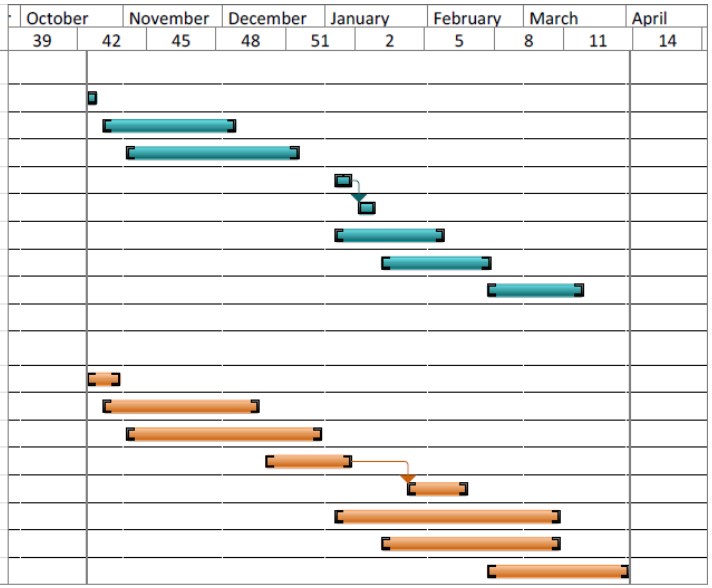

Time Schedule

Appendix B Theoretical and True Plate Angle

Theoretical and true plate angleRadius (mm)	Difference between theoretical and true plate angle (deg.)
$r_2 + 0.25$	2.3
$r_2 + 0.25$	2
$r_2 + 0.25$	1.8
$r_2 + 0.25$	1.4
$r_2 + 0.25$	1.5
$r_2 + 0.25$	4.3
r_3	5
r_3	4
r_3	33
r_3	1.5
$r_3 + 0.25$	6.5
$r_3 + 0.25$	4
$r_3 + 0.25$	2.5
$r_3 + 0.25$	2
$r_3 + 0.25$	2